

Gaussian continuous tensor network states: short-distance properties and imaginary-time evolution

Marco Rigobello

*Max-Planck-Institut für Quantenoptik, Hans-Kopfermann-Str. 1, D-85748 Garching, Germany and
Dipartimento di Fisica e Astronomia “G. Galilei”, Università di Padova, I-35131 Padova, Italy*

Erez Zohar

School of Physics and Astronomy, Tel Aviv University, Tel Aviv 6997801, Israel

We study Gaussian continuous tensor network states (GCTNS) — a finitely-parameterized subclass of Gaussian states admitting an interpretation as continuum limits of discrete tensor network states. We show that, at short distance, GCTNS correspond to free Lifshitz vacua, establishing a connection between certain entanglement properties of the two. Two schemes to approximate ground states of (free) bosonic field theories using GCTNS are presented: rational approximants to the exact dispersion relation and Trotterized imaginary-time evolution. We apply them to Klein-Gordon theory and characterize the resulting approximations, identifying the energy scales at which deviations from the target theory appear. These results provide a simple and analytically controlled setting to assess the strengths and limitations of GCTNS as variational ansätze for relativistic quantum fields.

I. INTRODUCTION

Tensor network states (TNS) [1, 2] are powerful tools for studying strongly correlated quantum systems. They have contributed to important analytical insights, such as the classification of symmetry-protected and topological phases of matter [3], and have broad numerical applications [4, 5]. By parametrizing many-body wavefunctions as contractions of low-rank tensors along virtual spaces, TNS capture the entanglement structure of local lattice models with resources that grow only polynomially with the system size, making them highly effective as variational classes. The most prominent example is the matrix product state ansatz (MPS) [6, 7], which underlies the density-matrix renormalization group [8–10] and provides quasi-exact results for one-dimensional models. Projected entangled-pair states (PEPS) [11] extend the MPS construction and its area-law entanglement to higher dimensions; although optimization is much more demanding, PEPS achieved state-of-the-art results, e.g. for the doped 2d Hubbard model [12]. Over the years, other ansätze have been introduced, such as tree tensor networks (TTN) [13] and the multi-scale entanglement renormalization ansatz (MERA) [14], especially tailored to critical phenomena [15].

TNS have long been employed also to study systems with a continuous number of degrees of freedom, described by quantum field theory (QFT). A prominent focus of this program has been on low-dimensional gauge theories [16], where TNS algorithms have enabled non-perturbative investigations of problems intractable for sampling methods [17], such as finite fermion density and out-of-equilibrium scenarios [18–20]. Like in Monte Carlo simulations, this is traditionally achieved by first discretizing the theory on the lattice, thereby introducing a short-distance cutoff, and finally extrapolating results to the continuum [21, 22]. It is nonetheless possible to formulate TNS directly in the continuum. Defining sparse variational manifolds capable of encoding QFTs at all length scales is both conceptually appealing and, potentially, computationally relevant, as it avoids delicate extrapolations in the lattice spacing. The breakthrough in this direction came with the introduction of continuous matrix product states (CMPS) [23], which realize a genuine continuum limit of MPS [24] and allow for the efficient computation of observables and variational gradients [25–27]. Generalization to higher dimensions required substantial efforts and led to continuous versions of PEPS [28] and MERA [29]. All these were later unified under the umbrella of continuous tensor network states (CTNS) [30], clarifying their origin as continuum limits of discrete TNS with the correct spatial symmetries [30, 31]. This limit has been recently constructed also for gauged PEPS [32], which span the Hilbert space of lattice gauge theories [33]. Crucially, while the one-dimensional CMPS retain a finite virtual space, consistency of the continuum limit in $d > 1$ demands infinite-dimensional virtual spaces [30], making the study of general CTNS virtually as challenging as the original QFT problems they were meant to solve. The Gaussian subclass (GCTNS), however, is analytically tractable by leveraging Wick’s theorem, and faithful descriptions of quadratic theories, as well as controlled approximations at weak coupling, have been worked out explicitly [31, 34].

In this work we analyze structural properties of Gaussian CTNS, focusing especially on their short-distance behavior. The main motivation for this analysis comes from relativistic QFT. In the relativistic setting, CMPS and CTNS are known to require an ultraviolet (UV) regulator to stabilize variational optimizations [34–37], reflecting their mismatch with the conformal short-distance behavior expected in relativistic QFTs and reintroducing the need for extrapolations. In $d = 1$, a relativistic modification of CMPS (RCMPS) remedies this by aligning the ansatz with the correct free-theory Fock structure [37, 38]. In higher-dimensional interacting theories, however, divergences are structurally more severe

and optimization will still require explicit cutoffs. In this regard, the Gaussian sector provides a valuable controlled setting to assess the strengths and limitations of continuous tensor network states beyond one space dimension [34].

The manuscript is organized as follows: Section II sets the notation by recalling the definition of CTNS and GCTNS, and briefly discusses the parent Hamiltonians and entanglement properties of the latter. In Section III we analytically construct approximate GCTNS ground states, thereby showing how Trotterized imaginary-time evolution can be interpreted as a CTNS. Section IV benchmarks these approximations against a free relativistic QFT, inspecting their UV properties. Section V summarizes our findings and discusses their implications, comparing to non-relativistic settings, CMERA and RCMPS.

II. CPEPS AND GAUSSIAN CPEPS

Consider a real scalar field operator $\hat{\phi}$ supported on d -dimensional space or, in the relativistic case, on a constant-time slice of $(d+1)$ -dimensional Minkowski spacetime. Introducing a basis of field configuration eigenstates,

$$\hat{\phi}(\mathbf{x})|\phi\rangle = \phi(\mathbf{x})|\phi\rangle, \quad (1)$$

any state $|\Psi\rangle$ of $\hat{\phi}$ may be identified with the Schrödinger wavefunctional $\Psi: \phi \mapsto \langle \phi | \Psi \rangle$. A CTNS or CPEPS [30, 31] for $\hat{\phi}$ is a state whose wavefunctional is expressed as a path integral over χ *auxiliary* or *virtual* fields [31]¹

$$\Psi(\phi) = \int \mathcal{D}\phi_1 \cdots \mathcal{D}\phi_\chi e^{-W(\phi, \phi_1, \dots, \phi_\chi; \mathbf{g})}, \quad (2)$$

where W is a *local* functional of the fields depending on a *finite* set of parameters \mathbf{g} , whose number, together with χ , controls the expressivity of the CTNS class². We further require W to be invariant under space rotations and translations. It has been shown that, with these assumptions, Ψ in Eq. (2) is the continuum limit of an ordinary PEPS whose auxiliary spaces correspond each to the (infinite-dimensional) Fock space of χ bosonic creation operators [30, 31]. In this sense, the number of auxiliary fields χ may be regarded as the field-theory analogue of the bond dimension. If the functional W' obtained integrating one virtual field, say ϕ_χ ,

$$e^{-W'(\phi, \phi_1, \dots, \phi_{\chi-1})} = \int \mathcal{D}\phi_\chi e^{-W(\phi, \phi_1, \dots, \phi_\chi)}, \quad (3)$$

is still local, W' also defines a CPEPS (with $\chi - 1$ virtual fields). Of course, virtually no closed-form solutions for QFT path-integrals such as the above are known, aside from Gaussian integrals and a few other very special exceptions.

In the Gaussian case (W quadratic in the fields), translation invariance makes it particularly convenient to work in momentum space. Collecting all the fields in $\phi = \{\phi_\alpha\}_{\alpha=0}^\chi$, with $\phi_0 = \phi$ the physical field, a GCPEPS with all the desired properties is obtained setting³ [31, 34]

$$W(\phi) = \frac{1}{2} \int d^d \mathbf{x} \phi(\mathbf{x})^\top [\mathbf{W}^{(0)} - \mathbf{W}^{(1)} \nabla^2] \phi(\mathbf{x}) = \frac{1}{2} \int \frac{d^d \mathbf{k}}{(2\pi)^d} \phi(-\mathbf{k})^\top \mathbf{W}(k) \phi(\mathbf{k}), \quad (4)$$

where $\mathbf{W}^{(0)}, \mathbf{W}^{(1)} \in \mathcal{M}_{\chi+1}(\mathbb{C})$ are constant symmetric matrices (the ansatz parameters \mathbf{g}), and $\mathbf{W}(k) = \mathbf{W}^{(0)} + \mathbf{W}^{(1)} k^2$ with $k = \|\mathbf{k}\|$. Fields and their Fourier transforms are denoted in the same way and we will often omit their \mathbf{x} or \mathbf{k} argument for brevity (they can be discerned from the integration measure), in which case $\bar{\phi}$ denotes $\phi(-\mathbf{k})$. In principle W could include terms constant and linear in ϕ ; however the former only affect the normalization and global phase of Ψ , which we are not going to keep track of, and linear terms can be reabsorbed by a constant shift of the fields. Of course the shift has physical consequences if ϕ_0 is involved; here we assumed $\langle \hat{\phi} \rangle_\Psi = 0$. Finally, higher-order derivatives of ϕ (i.e., letting \mathbf{W} be a finite polynomial of k^2) can be traded for additional virtual fields. More details on the general structure of W can be found in Appendices A and B.

Contracting the GCPEPS, i.e. integrating over the virtual fields, yields (up to normalization) the Gaussian state

$$\Psi(\phi) = \exp\left(-\frac{1}{2} \int \frac{d^d \mathbf{k}}{(2\pi)^d} \mathcal{K}(k) \bar{\phi} \phi\right), \quad (5)$$

¹The equivalence of this definition to that of Ref. [30] was proven in Ref. [31, Appendix A]. Generalization to curved spaces or systems with a boundary is possible [30]. In this work we only consider field theories on Euclidean \mathbb{R}^d and use the name CPEPS to stress this fact.

²That is, W is the space integral of a polynomial of a finite number of derivatives of the fields and functions of the fields values, all evaluated at the same position. In order to get a finite number of parameters \mathbf{g} , functions of the fields may be expanded in some finite basis set, e.g. a monomial basis [34].

³Fields are always assumed to satisfy suitable boundary conditions so that total derivatives can be discarded when integrating by parts.

with Gaussian kernel \mathcal{K} given by the Schur complement of the virtual ($\alpha, \beta > 0$) block $\mathbf{U}_{\alpha\beta}(k)$ in $\mathbf{W}_{\alpha\beta}(k)$ [31]

$$\mathcal{K} = \mathbf{W}_{00} - \sum_{\alpha, \beta=1}^{\chi} \mathbf{W}_{0\alpha} [\mathbf{U}^{-1}]_{\alpha\beta} \mathbf{W}_{\beta 0} . \quad (6)$$

The virtual fields propagator \mathbf{U}^{-1} can be written in terms of the adjugate matrix as

$$\mathbf{U}^{-1} = \frac{\text{adj } \mathbf{U}}{\det \mathbf{U}} . \quad (7)$$

Since the entries of \mathbf{W} are polynomials in k^2 , one concludes that n th-derivative GCPEPS with χ auxiliary fields are Gaussian states whose kernel \mathcal{K} is a *rational function* of k^2 of degree $n(\chi + 1)$ over $n\chi$ [31]. This property mirrors an analogous result for (discrete) Gaussian MPS [39]. Throughout this work, we will highlight some of its consequences. A first observation is that such a kernel (and thus the state Ψ) is specified by a number of parameters linear in χ , while the number of parameters in \mathbf{W} (and thus the GCPEPS ansatz) is quadratic in χ . This over-parameterization or “gauge” freedom is common in TNS constructions and can be removed bringing the ansatz in *canonical form*, often making numerical optimizations better conditioned [1]. We introduce below two canonical forms for first-order GCPEPS and refer to Appendix A for further details.

Let us first consider a diagonal virtual block and non-derivative physical-virtual couplings, setting

$$W(\phi) = \frac{1}{2} \int \frac{d^d \mathbf{k}}{(2\pi)^d} \left[(a + bk^2) \bar{\phi}_0 \phi_0 + \sum_{\alpha=1}^{\chi} (m_{\alpha} + k^2) \bar{\phi}_{\alpha} \phi_{\alpha} + 2i \sum_{\alpha=1}^{\chi} \sqrt{c_{\alpha}} \bar{\phi}_0 \phi_{\alpha} \right] . \quad (8)$$

Equation (6) then yields the linear partial fraction expansion

$$\mathcal{K}(k) = a + bk^2 + \sum_{\alpha=1}^{\chi} \frac{c_{\alpha}}{m_{\alpha} + k^2} , \quad (9)$$

which shows that it was not restrictive to normalize the virtual fields’ kinetic terms ($\mathbf{U}^{(1)} = \mathbf{I}$) in Eq. (8): $\mathbf{U}_{\alpha\alpha}^{(1)} \neq 1$ can be compensated for rescaling c_{α} and m_{α} , unless $\mathbf{U}_{\alpha\alpha}^{(1)} = 0$, in which case ϕ_{α} is spurious as it contributes a constant to \mathcal{K} , which can be adsorbed in a . Without loss of generality, we can further assume $c_{\alpha} \neq 0$ (otherwise ϕ_{α} decouples), and $m_{\beta} \neq m_{\alpha}$ for $\beta \neq \alpha$ (otherwise ϕ_{β} is redundant). With these assumptions, any rational \mathcal{K} having only simple poles, with numerator of degree at most $\chi + 1$ and denominator of degree exactly χ , can be uniquely written as Eq. (9) [40]. This is, in fact, the *generic* case; higher-order poles and sub-maximal degree denominators can nonetheless be recovered, e.g. taking \mathbf{U} in *symmetrized Jordan normal form* [41] and introducing some derivative couplings.

Another useful choice, which will naturally appear in the following, is to take \mathbf{W} *tridiagonal*. \mathcal{K} is easily computed integrating out virtual layers one by one, as per Eq. (3). The functional obtained integrating out $\phi_{\chi}, \dots, \phi_{\eta+1}$ reads

$$W^{(\eta)}(\phi_0, \dots, \phi_{\eta}) = \frac{1}{2} \int \frac{d^d \mathbf{k}}{(2\pi)^d} \left[\sum_{\alpha=0}^{\eta-1} u_{\alpha}(k) \bar{\phi}_{\alpha} \phi_{\alpha} + w_{\eta}(k) \bar{\phi}_{\eta} \phi_{\eta} + 2i \sum_{\alpha=1}^{\eta} v_{\alpha}(k) \bar{\phi}_{\alpha-1} \phi_{\alpha} \right] . \quad (10)$$

$W^{(\chi)} = W$ has this structure by hypothesis and Gaussian integration only updates the trailing main-diagonal coefficient:

$$w_{\eta} = u_{\eta} + v_{\eta+1}^2 / w_{\eta+1} , \quad w_{\chi} = u_{\chi} . \quad (11)$$

Iterating until $\eta = 0$, one gets the (finite) *continued fraction* (see also Ref. [42] for a direct computation of \mathbf{U}^{-1}),

$$\mathcal{K} = w_0 = u_0 + \cfrac{v_1^2}{u_1 + \cfrac{v_2^2}{\ddots + \cfrac{v_{\chi}^2}{u_{\chi}}}} . \quad (12)$$

Using the Euclidean algorithm (on $\mathbb{C}[k^2]$), *generic* rational functions of degree $\chi + 1$ over χ can be written in this way, with $v_{\alpha} = 1$ [43]. The convergence of continued fractions has been extensively studied [44], making this representation particularly convenient when discussing approximations of non-rational kernels \mathcal{K} by means of GCPEPS (Section III).

A. Parent Hamiltonians and renormalization

Key properties of a TNS can be understood through its parent Hamiltonians, namely (quasi-)local Hamiltonians that have the TNS as their ground state [45]. Ψ in Eq. (5) is the unique ground state of a family of Hamiltonians,

$$\hat{H}_\omega = \frac{1}{2} \int \frac{d^d \mathbf{k}}{(2\pi)^d} \frac{\omega(k)}{\text{Re } \mathcal{K}(k)} \left[\hat{\Pi}^\dagger \hat{\Pi} + |\mathcal{K}(k)|^2 \hat{\phi}^\dagger \hat{\phi} + \text{Im } \mathcal{K}(k) [\hat{\Pi}^\dagger \hat{\phi} + \hat{\phi}^\dagger \hat{\Pi}] \right], \quad (13)$$

parameterized by their (arbitrary) dispersion relation ω , and where $\hat{\Pi}$ is the conjugate momentum of $\hat{\phi}$. For simplicity, we assume time-reversal symmetry, i.e. $\text{Im } \mathcal{K} = 0$. Choosing ω appropriately, \hat{H}_ω can be taken local [31]. Instead, canonically normalizing the conjugate momentum term by setting $\omega = \mathcal{K}$, the class of GCPEPS is seen to encode *exactly* ground states (or vacua) of *free* scalar QFTs with dispersions rational in k^2 ,

$$\omega(k) = P(k^2)/Q(k^2), \quad (14)$$

with P, Q polynomials. Clearly, this is only a subset of all possible free QFTs; among the excluded models are all relativistic QFTs, which have

$$\omega(k) = \sqrt{m^2 + k^2}, \quad (15)$$

m being the field's mass. We will return to this point and study the faithfulness of various GCPEPS approximations of a free relativistic scalar field in Section IV. Provided Q in Eq. (14) has no zeros for $k^2 \geq 0$, \hat{H}_ω is still quasi-local, and it becomes local if Q is constant, in which case Ψ itself is a local *Rokhsar-Kivelson* wavefunctional, encoding the partition function of a d -dimensional statistical field theory [46–48]. A physically relevant example of local vacua is provided by free *Lifshitz* field theories [49, 50] with even dynamical exponent z , and certain massive deformations thereof [48]. Lifshitz models with $z \neq 1$ describe non-relativistic scale-invariant systems exhibiting anisotropic scaling between space and time, also known as Lifshitz scaling,

$$t \rightarrow \lambda^z t, \quad \mathbf{x} \rightarrow \lambda \mathbf{x}, \quad (16)$$

with $\lambda > 0$, implying

$$\omega(k) \propto |k|^z. \quad (17)$$

For a free Lifshitz scalar with positive even z , this gives a local vacuum wavefunctional represented by a GCPEPS with $\chi = 0$ and $(z/2)$ -order derivatives or, by Eq. (B4), $\chi = z/2 - 1$ and first-order derivatives.

The rational dispersion in Eq. (14) always approaches an even power of k at large momentum, hence GCPEPS look like even- z Lifshitz ground states at short-distance scales. In the language of the Wilsonian (momentum-shell) renormalization group (RG), the UV fixed point of an n th derivative GCPEPS with χ virtual fields is a free Lifshitz vacuum with

$$z = 2 \deg P - 2 \deg Q \leq 2n(\chi + 1). \quad (18)$$

Indeed, when acting on the quadratic wavefunctional Ψ , RG flow just rescales the couplings \mathbf{g} in \mathcal{K} according to their engineering dimension, therefore its Gaussian UV fixed point is the leading homogeneous piece of \mathcal{K} that dominates at large momenta [51]. Equation (18) is to be contrasted with relativistic QFTs, where Lorentz invariance implies $z = 1$ and the UV fixed point is expected to be a conformal field theory (CFT) [52].

B. Entanglement scaling

A defining property of ordinary (discrete) TNS is that the entanglement they can accommodate is bounded by some increasing function of the bond dimension χ . For instance, $S(A) \leq |\partial A| \log \chi$ for the entanglement entropy (EE) of a subsystem A , where $|\partial A|$ here denotes the area of the boundary in the TN geometry, i.e., the minimum number of virtual bonds that have to be cut in order to isolate A (e.g., $|\partial A| = 2$ for a bulk interval of an MPS) [3]. Whether CTNS obey analogous bounds with respect to the number of auxiliary fields is an open question [30]. The difficulty in answering it comes in part from the fact that EE is known to be UV divergent in QFT, where every finite patch of space hosts an infinite number of degrees of freedom [53, 54]. Consequently, *universal* (i.e., regularization-independent) entanglement quantifiers must be identified. Given a local QFT, regularized by means of a short-distance cutoff a , one expects the following $a \rightarrow 0$ expansion for the vacuum EE of a d -dimensional subregion [55]:

$$S = g_{d-1}(\partial A) a^{-(d-1)} + \dots + g_1(\partial A) a^{-1} - g_0(\partial A) \log(a) + S_0(A), \quad (19)$$

where $S_0(A)$ is finite and g_i are local functions of the entangling surface ∂A , which are homogeneous of degree i . The leading power-law divergences are unphysical (i.e., regularization-dependent), but the coefficient g_0 of the logarithmic divergence (if present) is expected to be regularization-independent and tied to the UV universality class of the QFT. The finite part S_0 also includes universal contributions which, however, are less straightforward to isolate [55].

As we just discussed, the UV fixed points of GCPEPS are free bosonic Lifshitz vacua with $z \leq 2n(\chi + 1)$. Their EE is expected to increase with z , as can be argued on the lattice based on the longer-range interactions arising from the discretization of higher-order derivatives [56]. In fact, CMERA predictions [57] and numerical observations [58] suggest a crossover from an area-law EE scaling at finite z , compatible with Eq. (19), to a volume law for $z \rightarrow \infty$. Whether this EE increase only inflates the leading divergence or also reflects on universal quantities (and if so, how) is not obvious in general. In one dimension, this question has been recently answered exploiting the Rokhsar-Kivelson structure of Lifshitz vacua: for a bulk interval and $z > 1$ [59]⁴,

$$g_0 = z - 1 \quad (20)$$

which grows with z as anticipated. This result implies that the EE of 1d GCPEPS⁵ has a logarithmic divergence whose coefficient is bounded by a linearly increasing function of χ . A numerical verification will be shown in Section IV C. In higher dimensions the landscape is more complex: in 2+1d exact analytical results for $z = 2$ show that EE has no logarithmic UV divergence for cuts across smooth entangling surfaces [61, 62] but corner singularities still produce universal log terms [48, 63]. Numerical investigations [58] indicate the same qualitative picture holds for $z > 2$; however, to our knowledge, monotonicity in z of the log-coefficient has not been established.

III. APPROXIMATING GROUND STATES

We now turn to the problem of finding an approximate CPEPS representation of the ground state of a given QFT. A well-established practice for TNS is to treat some CPEPS submanifold as a variational class over which to minimize the energy, e.g. via gradient descent [5, 10]. Variational optimization in the continuum has been successfully carried out using CMPS [23, 27] and RCMPS [64–66], as well as GCPEPS [34]. In what follows, we focus on two more specialized constructions, geared towards free theories and based on imaginary-time evolution or on the knowledge of a target dispersion relation. These will allow us to highlight analytically some properties of GCPEPS.

A. Rational approximants

Suppose a target dispersion relation ω is known — be it the exact dispersion of a free QFT or an effective one obtained using a Gaussian variational ansatz for the vacuum of an interacting QFT (Hartree approximation) [67–69]. The fidelity $F = |\langle \Omega | \Psi \rangle|^2$ between the associated Gaussian state Ω and the GCPEPS in Eq. (5) is essentially a measure of the functional distance between ω and \mathcal{K} : choosing as usual ϕ such that $\langle \hat{\phi} \rangle_\Omega = 0$,

$$\log F = V \int \frac{d^d \mathbf{k}}{(2\pi)^d} \log \frac{2\sqrt{\omega \mathcal{K}}}{\omega + \mathcal{K}} , \quad (21)$$

where V is a finite-volume regulator [31]. A first-derivative GCPEPS approximation of Ω with χ virtual fields can thus be obtained in two steps: (i) identify a rational approximant ω_χ of ω of degree $\chi + 1$ over χ in k^2 , e.g. via continued fraction or Padé approximation [31]; (ii) invert Eq. (6), namely solve it for \mathbf{W} with $\mathcal{K} = \omega_\chi$. A solution giving rise to a well-defined GCPEPS exists for any physically sensible ω_χ , but it is not unique due to gauge freedom (see Section A 1).

If a continued fraction approximation is employed for (i), the second step amounts to reading off the tridiagonal GCPEPS coefficients from Eq. (12). An example is the approximation of the $m > 0$ Klein-Gordon vacuum in Ref. [31], defined by

$$\{u_\alpha\}_{\alpha=0}^\chi = \{m, 2mk^2, 2m, 2mk^2, 2m, \dots\} , \quad v_\alpha = k^2 , \quad (22)$$

and corresponding to the continued fraction expansion of the relativistic dispersion relation centered at $k = 0$ and generated by recursion from the identity

$$\sqrt{m^2 + k^2} = m + \frac{k^2}{m + \sqrt{m^2 + k^2}} . \quad (23)$$

⁴ Although the bulk interval EE is IR-divergent for a massless Lifshitz scalar, $g_0 = -dS/d\log a|_{a=0}$ is independent of the system size L and, for $z = 2$, g_0 was also shown to be stable against massive deformations [48]. Both features follow the general expectation that long-distance features of a QFT should not affect its UV behavior and vice versa (no UV/IR mixing), and mirror the 1+1d relativistic case, where a Klein-Gordon field has the same EE scaling of a conformal boson and finite-size corrections are independent of a [60].

⁵Still equipped with infinite-dimensional virtual spaces, i.e., not a CMPS.

B. Imaginary-time evolution

The ground state Ω of a gapped Hamiltonian \hat{H} can also be obtained via imaginary-time evolution: for any state Ψ_0 having non-vanishing overlap with Ω , $e^{-T\hat{H}}|\Psi_0\rangle \sim \langle\Omega|\Psi_0\rangle e^{-TE_0}|\Omega\rangle$ when $T \rightarrow \infty$. Disregarding normalization issues and splitting the imaginary-time interval $[-T, 0]$ into N short segments,

$$|\Omega\rangle = \lim_{T \rightarrow \infty} \lim_{N \rightarrow \infty} \int \mathcal{D}\phi_0 \cdots \mathcal{D}\phi_N |\phi_0\rangle \langle\phi_0| e^{-(T/N)\hat{H}} |\phi_1\rangle \langle\phi_1| \cdots e^{-(T/N)\hat{H}} |\phi_N\rangle \langle\phi_N| \Psi_0 \rangle . \quad (24)$$

Comparing with Eq. (2), one is tempted to identify the path-integral above with a CPEPS with $\chi = N$. However, even for local Hamiltonians, the integrand is not the exponential of a local functional. The standard solution is to expand to first order in the Trotter step, $\epsilon = T/N \ll 1$. Assuming $\hat{H} = K(\hat{\Pi}) + V(\hat{\phi})$,

$$\langle\phi_{\alpha-1}|e^{-\epsilon\hat{H}}|\phi_\alpha\rangle \approx \int \mathcal{D}\Pi \langle\phi_{\alpha-1}|\Pi\rangle \langle\Pi| e^{-\epsilon K(\hat{\Pi})} e^{-\epsilon V(\hat{\phi})} |\phi_\alpha\rangle = \int \mathcal{D}\Pi e^{i \int d^d x \Pi [\phi_{\alpha-1} - \phi_\alpha] - \epsilon H(\Pi, \phi_\alpha)} . \quad (25)$$

For the usual case of $K = \int \Pi^2/2$, the functional integral over Π is just the value of the integrand at its stationary point. Plugging into Eq. (24) and formally setting $\Psi_0 = 1$, so that dependence on the initial state drops out, the path-integral takes the form in Eq. (2) with $\chi = N$ and

$$W(\phi) = \epsilon \sum_{\alpha=1}^N \left[\frac{1}{2} \int d^d x \left[\frac{\phi_{\alpha-1} - \phi_\alpha}{\epsilon} \right]^2 + V(\phi_\alpha) \right] = \epsilon \sum_{\alpha=1}^N H\left(\Pi = \frac{\phi_{\alpha-1} - \phi_\alpha}{\epsilon}, \phi = \phi_\alpha\right) . \quad (26)$$

Assuming H satisfies the usual properties (locality, translation and rotation invariance) which we required from a good CPEPS, Eq. (26) defines a family $\Omega_{N,\epsilon}$ of CPEPS approximations of Ω . Their virtual fields have the role of sampling physical field configurations at past imaginary times, and W intertwines only fields from subsequent time steps. Indeed, the approximation for a given N is obtained simply applying the imaginary-time propagator to $\Omega_{N-1,\epsilon}$:

$$\Omega_{N,\epsilon}(\phi) = \int \mathcal{D}\tilde{\phi} e^{-\epsilon H([\phi - \tilde{\phi}]/\epsilon, \tilde{\phi})} \Omega_{N-1,\epsilon}(\tilde{\phi}) , \quad \Omega_0 = \Psi_0 . \quad (27)$$

In the $T, N \rightarrow \infty$ limit, the usual path-integral representation of the QFT vacuum wavefunctional is recovered [55]⁶:

$$\lim_{T \rightarrow \infty} \lim_{N \rightarrow \infty} \Omega_{N,T/N}(\phi_0) = \int \mathcal{D}\varphi \exp \left[- \int_{-\infty}^0 d\tau H(\partial_\tau \varphi(\tau), \varphi(\tau)) \right] = \int \mathcal{D}\varphi e^{-S_E(\varphi)} , \quad (28)$$

where S_E is the Euclidean action and φ is now an Euclidean field, i.e. a function of both space and imaginary time.

For a free field with dispersion relation ω , in momentum space,

$$V(\phi) = \frac{1}{2} \int \frac{d^d k}{(2\pi)^d} \omega^2(k) \bar{\phi} \phi . \quad (29)$$

Equation (26) then defines a GCPEPS $\Omega_{N,\epsilon}$ with

$$W(\phi) = \frac{\epsilon^{-1}}{2} \int \frac{d^d k}{(2\pi)^d} \left[\bar{\phi}_0 \phi_0 + (2 + \epsilon^2 \omega^2(k)) \sum_{\alpha=1}^{N-1} \bar{\phi}_\alpha \phi_\alpha + (1 + \epsilon^2 \omega^2(k)) \bar{\phi}_N \phi_N - 2 \sum_{\alpha=1}^N \bar{\phi}_{\alpha-1} \phi_\alpha \right] . \quad (30)$$

The factorization $e^{-\epsilon\hat{H}} = e^{-\epsilon\hat{K}} e^{-\epsilon\hat{V}} + \mathcal{O}(\epsilon)$ used in Eq. (25) is clearly not unique. For instance, one could let the kinetic term act first, which amounts to exchanging the first and last diagonal coefficients in Eq. (30), or use a second-order Suzuki-Trotter decomposition. All such choices lead to the same $\epsilon \rightarrow 0$ limit, but they differ at finite ϵ (see Table I). Since the Hamiltonian is time-independent, the coefficients are uniform in the time bulk $1 < \alpha < N$. Moreover, since imaginary-time evolution only couples virtual fields at subsequent time steps, the resulting GCPEPS are always tridiagonal and Eq. (12) applies, with

$$\{\epsilon u_\alpha\}_{\alpha=0}^N = \{s_0, 2s, 2s, \dots, s_1\} , \quad \epsilon v_\alpha = i . \quad (31)$$

⁶ $\epsilon \sum_{\alpha=1}^N \rightarrow \int_{-T}^0 d\tau$, and $[\phi_{\alpha-1} - \phi_\alpha]/\epsilon \rightarrow \partial_\tau \varphi(\tau = -\alpha\epsilon)$.

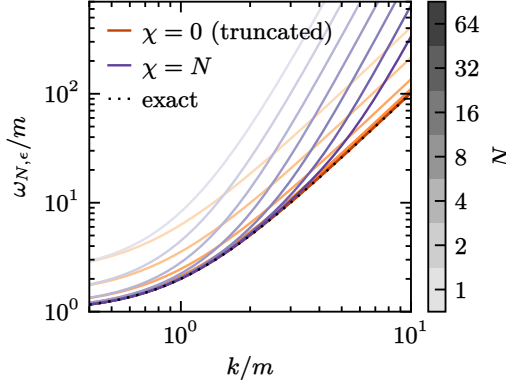


FIG. 1: Imaginary-evolution GCPEPS for a massive deformation of the $z = 2$ free Lifshitz field theory. Dispersions $\omega_{N,\epsilon}$ from a second-order Trotter decomposition with $mT = 4$, with and without truncating [Eq. (35) and (31) respectively]. The black dotted line depicts the exact dispersion $\omega(k) = m^2 + k^2$.

The coefficients s_0, s_1 are reported in Table I, and $s = (s_0 + s_1)/2 = 1 + \epsilon^2 \omega^2/2$. Convergence of the GCPEPS approximation is verified by recognizing in Eq. (31) the continued fraction expansion of a square root. To this aim, notice that ϵ prefactors amount to the rescaling $\mathcal{K} \rightarrow \epsilon^{-1} \mathcal{K}$, and u_N is irrelevant in the $N \rightarrow \infty$ limit (see Appendix C). Let $\omega_{N,\epsilon}$ be the Gaussian kernel \mathcal{K} associated with $\Omega_{N,\epsilon}$; assuming $\omega(k) \geq 0 \forall k$,

$$\lim_{\epsilon \rightarrow 0} \lim_{N \rightarrow \infty} \omega_{N,\epsilon} = \lim_{\epsilon \rightarrow 0} \epsilon^{-1} \left[\sqrt{s^2 - 1} + s_0 - s \right] = \omega \lim_{\epsilon \rightarrow 0} \left[\sqrt{1 + \frac{\epsilon^2 \omega^2}{4}} + C_1 \epsilon \omega \right] = \omega. \quad (32)$$

Here $C_1 = [s_0 - s]/\epsilon^2 \omega^2$ is a constant depending on the specific Trotter decomposition; for the second-order one $C_1 = 0$, and finite- ϵ corrections are $\mathcal{O}(\epsilon^2)$. Notice that here the order of the limits has been reversed with respect to Eq. (24), to simplify the derivation (see Appendix C for a justification).

Compressing the GCPEPS during imaginary-evolution

There is an important (yet expected) lesson to be learnt: as implemented above, without some compression scheme, imaginary-time evolution is not guaranteed to give the optimal CPEPS representation of a vacuum wavefunctional with the given χ . For instance, although vacua of free QFTs with dispersions rational in k^2 admit an exact GCPEPS representation with finitely many auxiliary fields, Eq. (30) produces an approximate GCPEPS for any finite χ and converges to the true ground state only in the $T, \chi \rightarrow \infty$ limit. This is exemplified in Fig. 1 for $\omega(k) = m^2 + k^2$, corresponding to a massive deformation⁷ of a free $z = 2$ Lifshitz field, and thus a $\chi = 0$ GCPEPS.

Standard TNS implementations of imaginary-time evolution, such as time-evolving block decimation [70, 71] or the time-dependent variational principle [72], feature a truncation/projection step to keep the state within some chosen TNS manifold and its bond dimension χ under control. Moreover, a well-conditioned optimization converges to the exact ground state if the latter admits an exact representation within the chosen manifold. The same holds for CPEPS, as we now demonstrate with a simple example, using again the $z = 2$ massive Lifshitz theory as a toy model.

To stay within a given CPEPS manifold during the evolution means that the state $\Omega_{N,\epsilon}$ keeps the form in Eq. (2) with a fixed functional W and, after each time step, only its parameters $\mathbf{g} = \mathbf{g}_N$ change. In the quadratic case, we can devise an update rule for GCPEPS combining a single Trotter step (Eq. 27), which in our notation amounts to

$$\epsilon \omega_{N,\epsilon} \rightarrow s_0 + [s_1 + \epsilon \omega_{N,\epsilon}]^{-1}, \quad (33)$$

with a rational approximation (Section III A). In the simplest example, $\chi = 0$, $\Omega_{N,\epsilon}$ is parameterized by $\mathbf{g}_N = (a_N, b_N)$ via

$$\omega_{N,\epsilon}(k) = a_N + b_N k^2. \quad (34)$$

⁷Lifshitz scaling implies the absence of a gap, preventing the convergence of imaginary-time evolution, however such massive deformation preserves the locality of Ω and has been considered in literature [48].

Approximating (truncating) the RHS in Eq. (33) with its second-order Maclaurin expansion in k^2 , we get⁸:

$$[\epsilon a_{N+1} - s_0(0)][\epsilon a_N + s_1(0)] = -1, \quad \frac{\epsilon b_{N+1} - \gamma[s_0(0) - 1]}{\epsilon b_N + \gamma[s_1(0) - 1]} = -\frac{\epsilon a_{N+1} - s_0(0)}{\epsilon a_N + s_1(0)}, \quad \gamma = \omega''(0)/\omega(0). \quad (35)$$

Setting $\Psi_0 = 1$ as usual, $a_0 = b_0 = 0$. Figure 1 shows that $\omega_{N,\epsilon} \rightarrow \omega$ even when the evolution is constrained within the $\chi = 0$ manifold, as expected. Coincidentally, since in this case the exact dispersion is completely characterized by $\omega(0)$ and $\omega''(0)$, the truncation actually accelerates convergence at high momenta.

IV. FREE RELATIVISTIC BOSON

The Klein-Gordon theory of a free scalar field is the simplest example of relativistic QFT. It provides the ideal playground for studying the pitfalls of approximating the relativistic dispersion relation with a rational function of k^2 . But first, what if one insists on realizing the relativistic dispersion through the parent Hamiltonian \hat{H}_ω in Eq. (13)?

A. Non-local field bases

Dropping the canonical normalization of the conjugate momentum in favor of $\omega(k) = \sqrt{m^2 + k^2}$, \hat{H}_ω in Eq. (13) is still *not* the Klein-Gordon Hamiltonian

$$\hat{H}_{\text{KG}} = \frac{1}{2} \int d^d \mathbf{x} \left[\hat{\Pi}^2 + (\nabla \hat{\phi})^2 + m^2 \hat{\phi}^2 \right]; \quad (36)$$

it is only equivalent to it through the *non-local* canonical transformation

$$\hat{\phi}(\mathbf{k}) = \sqrt{\frac{\mathcal{K}(k)}{\omega(k)}} \hat{\phi}_0(\mathbf{k}), \quad \hat{\Pi}(\mathbf{k}) = \sqrt{\frac{\omega(k)}{\mathcal{K}(k)}} \hat{\Pi}_0(\mathbf{k}), \quad (37)$$

where we now use $\hat{\phi}_0$ and $\hat{\Pi}_0$ for the original CPEPS fields. Substituting in Ψ from Eq. (5) replaces \mathcal{K} with ω :

$$\Psi(\phi) = \exp\left(-\frac{1}{2} \int d^d \mathbf{x} \phi(\mathbf{x}) \sqrt{m^2 - \nabla^2} \phi(\mathbf{x})\right). \quad (38)$$

Hence, a GCPEPS can encode Klein-Gordon's vacuum, just in a different field basis; however, no valid choice of \mathcal{K} can make the change of basis in Eq. (37) local because \mathcal{K} must be rational and ω is not. The Klein-Gordon field $\hat{\phi}(\mathbf{x})$ is then obtained from $\hat{\phi}_0(\mathbf{x})$ via convolution with a quasi-local kernel and, e.g., expectation values of field monomials $\langle \hat{\phi}^n(\mathbf{x}) \rangle$ and correlators $\langle \hat{\phi}(\mathbf{x}_1) \cdots \hat{\phi}(\mathbf{x}_n) \rangle$ translate into integrals of n -point functions for $\hat{\phi}_0(\mathbf{x})$, which can be evaluated directly from the CPEPS⁹. This is essentially how the RCMPS ansatz works, at least in its most naïve implementation [37]. Its “computational” field basis (or the higher-dimensional analogue) is the Fourier transform of the creation-annihilation pair $\hat{a}^\dagger(\mathbf{k}), \hat{a}(\mathbf{k})$ appearing in the mode expansion of $\hat{\phi}$,

$$\hat{a}(\mathbf{x}) = \int \frac{d^d \mathbf{k}}{(2\pi)^d} \sqrt{\frac{\omega(k)}{2}} \left[\hat{\phi}(\mathbf{k}) + \frac{i}{\omega(k)} \hat{\Pi}(\mathbf{k}) \right]. \quad (39)$$

Setting $\mathcal{K} = M$ with M some arbitrary energy scale, $\hat{a}^\dagger(\mathbf{x})$ and $\hat{a}(\mathbf{x})$ are nothing but the non-relativistic creation and annihilation operators for our CPEPS computational field:

$$\hat{\phi}_0(\mathbf{x}) = \sqrt{\frac{1}{2M}} [\hat{a}^\dagger(\mathbf{x}) + \hat{a}(\mathbf{x})], \quad \hat{\Pi}_0(\mathbf{x}) = i\sqrt{\frac{M}{2}} [\hat{a}^\dagger(\mathbf{x}) - \hat{a}(\mathbf{x})]. \quad (40)$$

The advantage of the RCMPS Bogoliubov basis is that it allows to straightforwardly normal order every operator, which in one dimension is enough to remove virtually all UV divergencies [37]. In higher dimensions, this is no longer the case and for interacting theories a cutoff is needed anyway. For this reason, here we refrain from performing any non-local field redefinition and instead study the GCPEPS approximations of the Klein-Gordon vacuum obtained following the constructions in Section III, characterizing their effective dispersion relations (Section IV B) and entanglement content (Section IV C).

⁸ $\omega'(0) = 0$ for a gapped real scalar field.

⁹For the free theory, one could define the CPEPS in \mathbf{k} -space, where the transformation in Eq. (37) is local, but ultimately the goal is to study interacting theories, where the Hamiltonian itself becomes non-local in momentum space.

rational $\mathcal{K} = \omega_\chi$ [Eq. (22)]		imaginary-evolution $\mathcal{K} = \omega_{N,\epsilon}$ [Eq. (31)]		
χ -odd	χ -even	$e^{-\epsilon\hat{K}}e^{-\epsilon\hat{V}} + \mathcal{O}(\epsilon)$	$e^{-\epsilon\hat{V}}e^{-\epsilon\hat{K}} + \mathcal{O}(\epsilon)$	$e^{-\epsilon\frac{\hat{V}}{2}}e^{-\epsilon\hat{K}}e^{-\epsilon\frac{\hat{V}}{2}} + \mathcal{O}(\epsilon^2)$
s_0		1	$1 + \epsilon^2\omega^2$	$1 + \epsilon^2\omega^2/2$
s		$1 + \epsilon^2\omega^2/2$
s_1		$1 + \epsilon^2\omega^2$	1	$1 + \epsilon^2\omega^2/2$
Λ (UV)	$m\chi$	$m\chi$	$1/\epsilon$	$1/\epsilon$
$\mathcal{K}(k \gg \Lambda)$	$k^2/m(\chi + 1)$	$m(\chi + 1)$	$1/\epsilon$	ϵk^2
μ (IR)	0	0	$\sqrt{1 - T^2 m^2}/T$...
$\mathcal{K}(k \ll \mu)$	—	—	$T(m^2 + k^2)$...

TABLE I: Coefficients, asymptotes, and domain of convergence of rational and imaginary-time GCPEPS approximants \mathcal{K} of Klein-Gordon's dispersion relation ω . The approximation's IR and UV scales, μ and Λ , are obtained by matching the corresponding asymptote of \mathcal{K} to ω , so that $\mathcal{K}(k) \approx \omega(k)$ for $\mu \ll k \ll \Lambda$. In the imaginary-time case, different Suzuki-Trotter decompositions are considered (all equivalent in the IR).

The rational approximant reproduces ω in the IR all the way down to $k = 0$.

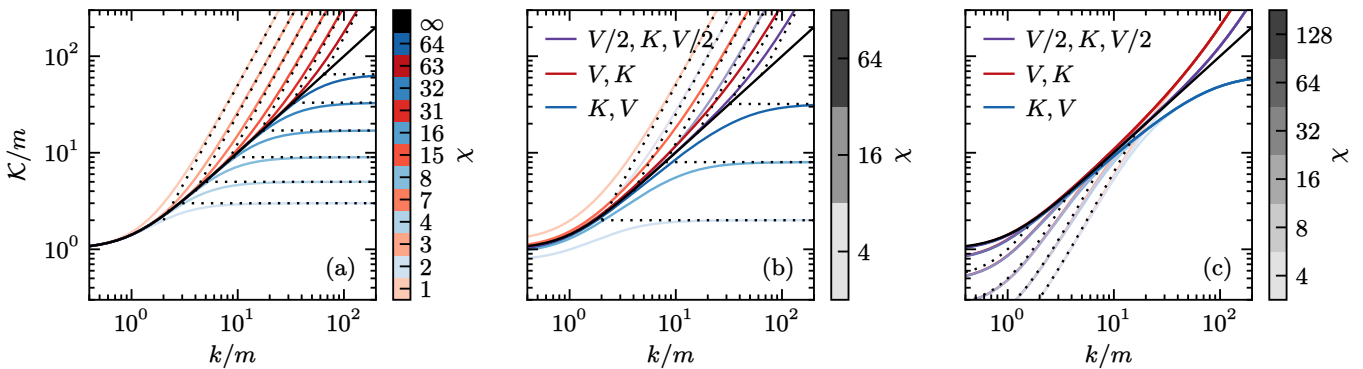


FIG. 2: (a) rational [Eq. (22)] and (b),(c) imaginary-time [Eq. (31)] GCPEPS approximants \mathcal{K} of the Klein-Gordon dispersion relation ω (black line) for different number χ of auxiliary fields. In (b) and (c), different colors denote different decompositions, while darker lines correspond to larger χ . Dotted lines represent the asymptotes in Table I. In (b), the evolution time $mT = 2$ is fixed and the Trotter step $m\epsilon = mT/\chi \in \{1/2, \dots, 1/32\}$ shrinks with χ . In (c), $m\epsilon = 1/64$ is fixed and $mT = m\epsilon\chi \in \{1/16, \dots, 2\}$; notice that all decompositions overlap in the IR, visually matching the exact dispersion for $mT \gtrsim 2$.

B. Effective dispersion relations

Figure 2 compares the exact Klein-Gordon dispersion in Eq. (15) with its finite- χ approximants ω_χ and $\omega_{N,\epsilon}$ from Eqs. (22) and (31), which we refer to as rational and imaginary-evolution approximations, respectively¹⁰. As expected, all approximations improve (exponentially) for larger χ , but convergence is not uniform [31]: errors generally increase with larger momenta or smaller masses. A more detailed convergence analysis can be found in Appendix C, while we focus on the asymptotic behavior of the approximants. The results are summarized in Table I.

The rational approximation converges by monotone oscillation, and qualitatively different behaviors arise for even χ (blue lines in Fig. 2a, converging from below) and odd χ (red, above) when $k \gg m$:

$$\omega_\chi \sim \begin{cases} k^2/m(\chi + 1) & \text{for } \chi \text{ odd} \\ m(\chi + 1) & \text{for } \chi \text{ even} \end{cases} ; \quad (41)$$

¹⁰The labelling is just for convenience. Both dispersions are rational functions, as per Eq. (14).

as can be checked by induction, recalling $\omega_0 = m$, $\omega_1 \sim k^2/2m$ and using

$$\omega_{\chi+2} = m + \frac{k^2}{2m + \frac{k^2}{m + \omega_\chi}}. \quad (42)$$

Comparing Eq. (41) with the exact dispersion suggests that the continued fraction approximation breaks down at the energy scale $\Lambda \approx m\chi$, which is confirmed also by Fig. 2a.

Analogous results hold for imaginary-evolution ground states: for any finite $\chi = N$ and ϵ , the effective dispersion $\omega_{N,\epsilon}$ is a rational function of k^2 and thus accurately reproduces the exact one only on a finite momentum window. As expected, this window grows with larger imaginary-time intervals T , finer Trotter steps ϵ , and higher-order decompositions (see Figs. 2b and 2c). The asymptotes of $\omega_{N,\epsilon}$ are once again found by induction and matched to the exact dispersion ω to estimate the domain of convergence. In this case $\omega_{N=0,\epsilon} = s_0/\epsilon$, and expanding Eq. (33) for $\epsilon\omega \gg 1$ shows that $\omega_{N,\epsilon} \sim s_0/\epsilon$ in the UV ($k \gg 1/\epsilon$), independently of N . That is, the UV properties of the CPEPS are fully determined by the last Trotter step. The UV behavior is thus controlled by ϵ and the Trotter decomposition order (Fig. 2c), with the second-order decomposition achieving the same precision as the first-order ones with the same T and half the Trotter steps N . Differently from the rational case, the imaginary-evolution approximation is not centered in $k = 0$; rather, T controls its quality in the infrared (IR): $\omega_{N,\epsilon} \sim T\omega^2$ for $T\omega \ll 1$, and only when $Tm \gtrsim 1$ is the cutoff effectively removed (Fig. 2b). This result follows immediately also from Eq. (C12). We stress that these two asymptotes are general and apply to any quadratic Hamiltonian, such as the massive Lifshitz one of Fig. 1. Their prediction for Klein-Gordon is reported in Table I.

Ultimately, an infinite number of high-frequency modes are misrepresented by any finite- χ GCPEPS for Klein-Gordon because a rational function of k^2 can never reproduce the relativistic asymptotics $\omega \sim k$. Similarly to a lattice regularization, the approximations derived above still accurately capture the low-energy, long-distance properties of the field theory and implicitly introduce a soft UV cutoff Λ . If the ground state was to be found variationally, however, an explicit cutoff of some sort would be needed for convergence [35–38].

C. Entanglement entropy

We showed above that finite- χ GCPEPS approximations fail to reproduce the ultraviolet behavior of Klein-Gordon; we thus do not expect them to capture the correct scaling limit of the EE S . Alternatively, in light of Section IV A, this mismatch can also be argued on the grounds that the GCPEPS represents the exact Klein-Gordon vacuum in a non-local field basis. Since all terms in Eq. (19) specific to $d > 1$ are regularization dependent, a first meaningful check can be carried out already in one spatial dimension. For a 1+1d relativistic QFT, g_0 is proportional to the central charge c of its UV fixed point CFT and, for a large enough bulk interval A [53, 60],

$$S \sim \frac{c}{3} \log(\xi/a) \quad \text{when } |A| \gg \xi \gg a, \quad (43)$$

where $\xi = 1/m$ is the correlation length. For a massless scalar $c = 1$, corresponding to $g_0 = 1/3$. We expect the GCPEPS ground states to match this result up to the scale $1/a \approx \Lambda$, at which the approximation breaks down¹¹; beyond that, the scaling will be ruled by the effective GCPEPS dispersion. Two asymptotic behaviors were found above, corresponding to $\mathcal{K}(k) \sim \gamma k^z$ for some constant $\gamma > 0$ and $z = 0$ or $z = 2$. The first case of an asymptotically flat dispersion implies that high-energy modes are completely localized and thus do not contribute to the entanglement: the UV fixed point is trivial. The second case corresponds in the UV to a $z = 2$ Lifshitz scalar, for which (in $d = 1$) Eq. (20) gives $g_0 = z - 1 = 1$. In summary, when $\xi, |A| \gg a$ we anticipate:

$$g_0^{\text{eff}}(a) = -a \frac{dS}{da} \approx \begin{cases} 0 & \text{for } a \ll \Lambda^{-1} \text{ and } z = 0 \\ 1/3 & \text{for } \Lambda^{-1} \ll a \quad (z = 1) \\ 1 & \text{for } a \ll \Lambda^{-1} \text{ and } z = 2 \end{cases}; \quad (44)$$

with $g_0 = \lim_{a \rightarrow 0} g_0^{\text{eff}}(a) \in \{0, 1\}$. In what follows we verify this claim numerically, introducing a lattice regularization.

¹¹We recall $\Lambda = \mathcal{O}(m\chi)$ for the rational approximations, and $\Lambda = \mathcal{O}(\chi/T)$ for the imaginary-evolution ones.

The EE of a free lattice boson can be computed following the real-time approach of Ref. [55] (correlator method): For a Gaussian state, the reduced density matrix of a subsystem A can be expressed solely in terms of 2-point functions involving $\hat{\phi}_x$ degrees of freedom situated inside A. Its Von Neumann entropy (the EE of A) reads

$$S = \text{tr} \left(\frac{\mathbf{C} + 1}{2} \log \frac{\mathbf{C} + 1}{2} - \frac{\mathbf{C} - 1}{2} \log \frac{\mathbf{C} - 1}{2} \right), \quad \mathbf{C} = \sqrt{[\mathcal{K}^{-1}]_A \mathcal{K}_A}, \quad \frac{1}{2} [\mathcal{K}^{-1}]_{xy} = \langle \hat{\phi}_x \hat{\phi}_y \rangle; \quad (45)$$

where \mathcal{K} is the inverse covariance matrix (or position-space kernel) of the state, and \mathcal{K}_A denotes its restriction to $\mathbf{x}, \mathbf{y} \in A$. For our GCPEPS approximations, \mathcal{K}_{xy} is the discrete Fourier transform of $\mathcal{K}(k)$, up to lattice artifacts. We consider a periodic chain of length L and spacing a and set:

$$\mathcal{K}_{xy} = \frac{1}{L} \sum_{\mathbf{k}} e^{i\mathbf{k} \cdot (\mathbf{x} - \mathbf{y})} \mathcal{K}(\tilde{k}), \quad \tilde{k}^2 = \left\| \frac{2}{a} \sin \frac{a\mathbf{k}}{2} \right\|^2 = k^2 [1 + \mathcal{O}(ak)^2], \quad \mathbf{k} \in \frac{2\pi}{L} \mathbb{Z}_{L/a}; \quad (46)$$

which corresponds to replacing ∇^2 by the finite-difference Laplacian. However, numerically we find that using \tilde{k} or k does not alter g_0 , as expected for a regularization-independent quantity. The bulk EE scaling is similarly not affected by finite-size effects or the choice of boundary conditions, justifying the introduction of a finite-volume regularization (see also footnote 4).

Figure 3 shows the EE as given by Eq. (45) for different bipartitions of the ring, as a function of their chord length:

$$\ell(|A|) = \ell(L - |A|) = \frac{L}{\pi} \sin \frac{\pi|A|}{L}. \quad (47)$$

With the regulator a in place, GCPEPS representations with $\mathcal{K} \sim \gamma k^z$ converge to the exact curve (black) for increasing χ — from below or above for $z = 0$ and $z = 2$, respectively. On the other hand, using a symmetric bipartition as a reference, Fig. 4 clearly shows that the continuum scaling of the GCPEPS EE is different from the exact one and g_0^{eff} , shown in Fig. 5 (a), matches the prediction in Eq. (44). Importantly (and as predicted), the correct Klein-Gordon scaling still emerges in the $\Lambda^{-1} \ll a \ll \xi$ regime, preceding the breakdown of the GCPEPS approximation. In Fig. 5 (b) we demonstrate this by extrapolating $g_0 = 1/3$ to 3-digit precision from rational approximations. We focus on even χ GCPEPS, for which $g_0^{\text{eff}}(a; \chi)$ has a maximum at finite $a = a_{\chi}^*$, such that $a_{\chi}^* \rightarrow 0$ for $\chi \rightarrow \infty$. Finding the maximum is a unimodal search problem on integers (because of the lattice) which can be efficiently solved using a binary search. By fitting the maxima of different χ curves as a function of their location a_{χ}^* to a degree-3 polynomial and extrapolating to $a_{\chi}^* = 0$, we obtain $g_0^{\text{eff}}(a=0; \chi=\infty) = 0.3334(2)$. The details of the interpolation procedure are reported in the Figure's caption. A rather large number of virtual fields is required for a precise extrapolation; this is not surprising given that the central charge is a UV property of the theory.

V. CONCLUSION

Gaussian continuous tensor network states (GCPEPS) encode ground states of quadratic quantum field theories whose dispersion relations ω are rational functions of k^2 , and that thus flow in the UV to free Lifshitz field theories with even dynamical exponent z . When the GCPEPS has a tridiagonal structure, we showed that ω has a natural representation as a continued fraction; generalization to block tridiagonal matrices should be possible [74]. In contrast with CMPS and Gaussian CMERA, which have a UV-finite entanglement entropy [75, 76], we find that the entanglement entropy is generally divergent for the (broader) GCTNS class studied here. Its UV scaling matches that of Lifshitz ground states. In one dimension, this manifests as a logarithm of the UV regulator multiplied by a universal coefficient bounded by a linearly growing function of the number of auxiliary fields χ . We verified this result numerically with some examples. In higher dimensions, entanglement scaling in Lifshitz theories with arbitrary dynamical exponent is yet to be fully characterized, but there is ongoing progress in this direction [56–59, 77–79], and future studies may further elucidate the entanglement content of GCTNS, at least as far as continuum scaling is concerned.

Another consequence of a dispersion rational in k^2 is that GCPEPS cannot capture the short-distance properties of relativistic quantum field theories *asymptotically*, such as their linear dispersion and entanglement scaling. We studied this limitation quantitatively in the simple setting of Klein-Gordon field theory. To this aim, we first showed how to approximate ground states by means of GCPEPS using rational approximants or Trotterized imaginary-time evolution. The latter yields a tridiagonal GCPEPS whose auxiliary fields can be interpreted as snapshots of past (imaginary) times. Using a toy example, we showed how to compress this conceptually appealing but inefficient representation, disentangling the number of auxiliary fields from the number of Trotter steps. Although in this work we focused on free theories, real and imaginary-time evolution can be extended to interacting Hamiltonians by devising a scheme

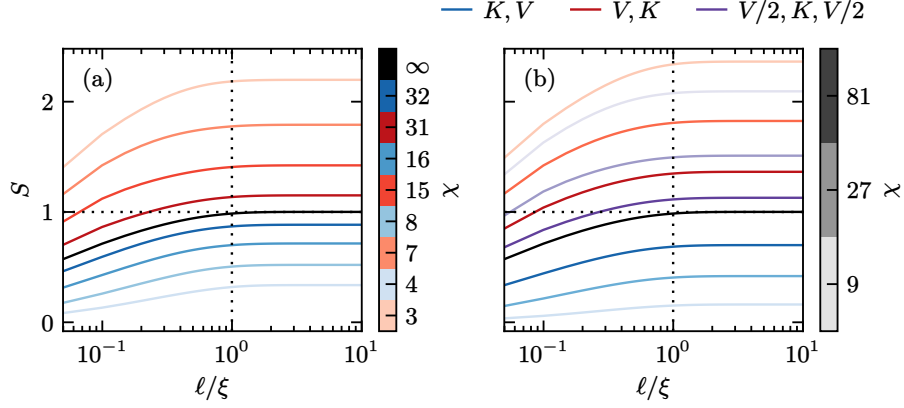


FIG. 3: Lattice-regularized EE $S(\ell)$ of the exact Klein-Gordon vacuum on a ring (black curve), and of its (a) rational and (b) $mT = 4$ imaginary-time GCPEPS approximations. Regulators: $a/\xi = e^{-3} \approx 0.05$, $L/\xi \approx 10\pi$ (closest integer multiple of a/ξ). The black curve shows the exact (regularized) EE. Dotted grid lines mark $\ell(\xi) \approx \xi$ (vertical) and $S = (1/3) \log(\xi/a) = 1$ (horizontal).

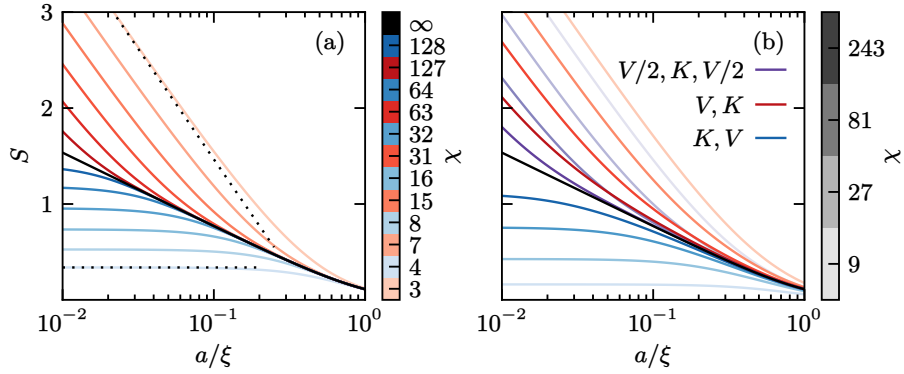


FIG. 4: Continuum scaling of the EE from Fig. 3 (a) and (b), for a symmetric bipartition ($|A| = L/2$). Dotted lines in (a) show sample scalings with $g_0 \in \{0, 1\}$, matching even- and odd- χ rational GCPEPS approximations in the $a \ll 1/\Lambda$ domain.

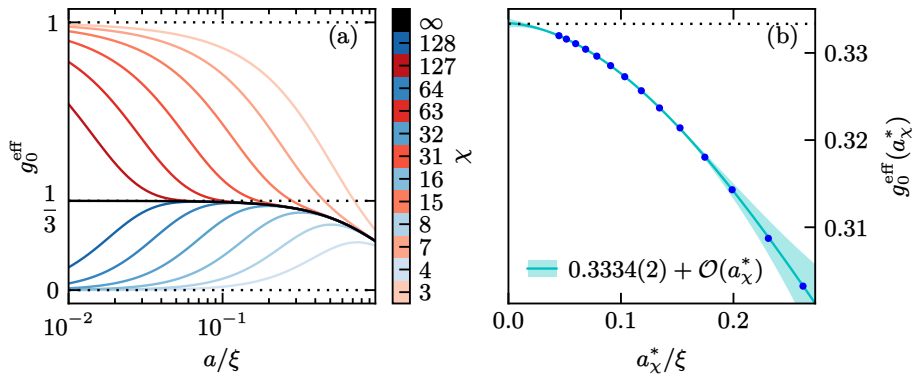


FIG. 5: (left) log a -derivative g_0^{eff} of the EE scalings in Fig. 4 (a); (right) g_0^{eff} peaks for 14 log-spaced even $\chi \in \{22, 26, \dots, 216\}$ (blue points) and their cubic polynomial interpolation with its 3σ confidence belt (light blue area). The intercept, corresponding to $\chi \rightarrow \infty$, is compatible with Klein-Gordon's $g_0 = 1/3$ (dotted line). To suppress (and estimate) the dependence of the extrapolation on the choice of fitting window, multiple fits are performed, one for each subinterval containing the $n \geq 7$ largest- χ data points. Average and standard deviation of the constant term are reported in the legend. The polynomial degree was chosen by minimizing the AICc (Akaike information criterion, corrected for small sample sizes [73]).

to ensure that the evolved state remains inside the (G)CPEPS manifold, e.g. in the spirit of the time-dependent variational principle [72, 80].

Both the rational and imaginary-time evolution approximations above accurately reproduce the low-energy properties of Klein-Gordon while effectively introducing a high-energy scale beyond which the approximation breaks down, as expected. This soft cutoff is raised by adding more auxiliary fields and, with χ large enough, even ultraviolet quantities can be accurately extrapolated, as we demonstrated computing the central charge of the free relativistic massless boson. However, the number of virtual fields we used for the extrapolation is much larger than those in previous numerical CTNS studies [34] and variational computations in interacting theories might become impractical for such large χ . Additionally, the emergence of a cutoff partially defeats the purpose of introducing *continuous* tensor network states in the first place [37], namely offering a description of the field theory valid at *all scales*. Regrettably, GCPEPS approximations of relativistic quantum fields achieve the latter only for $\chi = \infty$.

A similar problem to the one just outlined has already been faced in one space dimension, where CMPS [23] provide a consistent continuum TNS ansatz with finite-dimensional virtual spaces [30], thus allowing for variational optimization beyond Gaussianity, but are not adapted to the UV behavior of relativistic theories. RCMPS (relativistic CMPS) [37] solve the problem by expanding the state in a basis of *quasi-local* real-space degrees of freedom. In this way, the correct conformal short-distance behavior is inbuilt into the ansatz. In fact, we re-derived the RCMPS field basis from GCPEPS using the sole requirement of reproducing the relativistic dispersion. While the approach can be extended to higher dimensions, crucial to the success of RCMPS is the fact that, in $1+1d$ relativistic QFTs, normal ordering is generally enough to cure all UV divergencies [37]. For interacting theories in higher dimensions, however, this is no longer true. In the presence of UV divergencies, variational optimization will adjust the variational parameters toward fitting shorter and shorter distances, which dominate the energy density, paradoxically degrading the accuracy at physical length scales [38, 81]. Nevertheless, before RCMPS were introduced, CMPS had been successfully combined with an explicit UV cutoff to study relativistic theories, proving this is a viable approach [35, 36]. On the one hand, by clarifying the scales at play in the approximation, this work can therefore inform future (G)CTNS investigations of interacting relativistic QFTs with a cutoff. On the other hand, by stressing certain limitations of the ansatz, we highlight the need for new methods tailored to relativistic contexts, mirroring what the RCMPS achieved in one space dimension.

ACKNOWLEDGMENTS

We are grateful to Tom Shachar for his insightful contributions to the initial development of this work. We thank Antoine Tilloy, Erickson Tjoa, Gertian Roose and Niranjan Kumar for helpful discussions. MR thanks the Racah Institute of Physics of the Hebrew University of Jerusalem for hospitality and partial support. This work has received funding from the European Union under the Horizon Europe research and innovation programme through the project PASQuanS2.1 (grant agreement No. 101113690) and from the ERC project OverSign (grant agreement No. 101122583). Views and opinions expressed are however those of the author(s) only and do not necessarily reflect those of the European Union or the European Research Council. Neither the European Union nor the granting authority can be held responsible for them. Work at MPQ is part of the Munich Quantum Valley, which is supported by the Bavarian state government with funds from the Hightech Agenda Bayern Plus.

Appendix A: GCPEPS canonical forms

As anticipated in Section II, the quadratic first-order GCPEPS functional W in Eq. (4) is largely over-parameterized:

$$\mathbf{W}(k) = \mathbf{W}^{(0)} + \mathbf{W}^{(1)}k^2, \quad (\text{A1})$$

with $\mathbf{W}^{(i)} \in \mathcal{M}_{\chi+1}(\mathbb{C})$ symmetric, contains $(\chi+1)(\chi+2)$ complex parameters, while the physical state, specified by

$$\mathcal{K}(k) = \frac{P^{(\chi+1)}(k^2)}{Q^{(\chi)}(k^2)}, \quad (\text{A2})$$

has only $2\chi+2$.

We defined two “canonical forms” for GCPEPS: symmetrized Jordan \mathbf{U} and tridiagonal \mathbf{W} — corresponding respectively to *flat* (all ϕ_α couple directly only to ϕ_0) and *nested* (each ϕ_α couples to $\phi_{\alpha\pm 1}$) physical-virtual couplings. The first form can encode *any* translation and rotation invariant first-order GCPEPS; the latter has useful $\chi \rightarrow \infty$ convergence properties and, by analytic continuation, covers *generic* GCPEPS, i.e. \mathbf{W} or \mathcal{K} picked at random. We

now show how \mathbf{W} is brought into such forms and specify which rational Gaussian kernels \mathcal{K} can arise from each, but first we shall set the notation and recall some basic facts about the convergence of Gaussian path-integrals [82].

For the present purposes, it is convenient to isolate the physical field $\phi = \phi_0$ from the virtual multiplet $\varphi = \{\phi_\alpha\}_{\alpha=1}^\chi$. Accordingly, we parameterize

$$\mathbf{W} = \begin{bmatrix} u & \mathbf{v}^\top \\ \mathbf{v} & \mathbf{U} \end{bmatrix}, \quad (\text{A3})$$

and analogously for each $\mathbf{W}^{(i)}$, $i \in \{0, 1\}$, with

$$u^{(i)} \in \mathbb{C}, \quad \mathbf{v}^{(i)} \in \mathbb{C}^\chi, \quad \mathbf{U}^{(i)} = \mathbf{U}^{(i)\top} \in \mathcal{M}_\chi(\mathbb{C}). \quad (\text{A4})$$

Carrying out the Gaussian integral

$$\Psi(\phi) = \int \mathcal{D}\varphi e^{-W(\phi, \varphi)} = \exp\left(-\frac{1}{2} \int \frac{d^d \mathbf{k}}{(2\pi)^d} u(k) \bar{\phi} \phi\right) \int \mathcal{D}\varphi \exp\left(-\int \frac{d^d \mathbf{k}}{(2\pi)^d} \left[\frac{1}{2} \bar{\varphi}^\top \mathbf{U}(k) \varphi + \bar{\varphi}^\top \mathbf{v}(k) \phi\right]\right), \quad (\text{A5})$$

one readily obtains Eq. (6), namely

$$\mathcal{K} = u - \mathbf{v}^\top \mathbf{U}^{-1} \mathbf{v}. \quad (\text{A6})$$

The path-integral formally (i.e., mode-by-mode) converges iff the Hermitian part $\text{Re } \mathbf{U}(k)$ of $\mathbf{U}(k)$ is positive definite (as a real matrix) $\forall k$, i.e. iff

$$\text{Re } \mathbf{U}^{(0)} \succ 0 \text{ and } \text{Re } \mathbf{U}^{(1)} \succeq 0; \quad (\text{A7})$$

implying that, as a rational function on the complex k^2 plane, \mathcal{K} has no singularities for (physical) $k^2 \geq 0$.

Proof. Poles of \mathcal{K} are contained in the zeros of $\det \mathbf{U}$ and, for \mathbf{U} complex symmetric, $\text{Re } \mathbf{U} \succ 0 \Rightarrow \mathbf{U}$ is non-singular. \square

Since

$$\|\Psi\|^2 = \int \mathcal{D}\phi |\Psi(\phi)|^2 = \int \mathcal{D}\phi \exp\left(-\int \frac{d^d \mathbf{k}}{(2\pi)^d} \phi(-\mathbf{k}) \text{Re } \mathcal{K}(k) \phi(\mathbf{k})\right), \quad (\text{A8})$$

Ψ is formally normalizable iff, moreover, $\text{Re } \mathcal{K}(k) > 0 \forall k$. By a property of the Schur complement [83, Proposition 16.1],

$$\text{Re } \mathbf{U} \succ 0 \text{ and } \text{Re } \mathcal{K} > 0 \iff \text{Re } \mathbf{W} \succ 0. \quad (\text{A9})$$

In the following we explicitly enforce Eq. (A7) but not Eq. (A9). We also note that at $k = 0$ positive definiteness is often relaxed to positive semi-definiteness (with an implicit regulator), to accommodate for “massless” modes.

The GCPEPS “gauge” freedom, by which we aim to put \mathbf{W} in canonical form, consists of transformations that leave ϕ and \mathcal{K} unchanged and respect the GCPEPS structure. These correspond to local linear auxiliary-field redefinitions,

$$\varphi \rightarrow \mathbf{R}\varphi + \mathbf{s}\phi, \quad (\text{A10})$$

with \mathbf{k} -independent $\mathbf{R} \in \text{GL}(\chi, \mathbb{C})$ and $\mathbf{s} \in \mathbb{C}^\chi$. Equation (A10) clearly preserves Gaussianity and the path-integral measure $\mathcal{D}\varphi(\mathbf{k})$ (up to a constant) but, when \mathbf{R} or \mathbf{s} have non-real entries, one should in principle regard each $\varphi(\mathbf{k})$ integral after the transformation as a contour integral over a tilted and shifted real hyperplane in \mathbb{C}^χ . Nevertheless, provided the transformed virtual block,

$$\mathbf{U}' = \mathbf{R}^\top \mathbf{U} \mathbf{R}, \quad (\text{A11})$$

still satisfies $\text{Re } \mathbf{U}' \succ 0$, the contour can be deformed back to real φ .

1. Symmetrized Jordan normal form

Any GCPEPS can be written using a symmetrized Jordan [41] block diagonal \mathbf{U} , and k -dependence as follows:

$$\mathbf{W}(k) = \begin{bmatrix} a + bk^2 & k^2 \mathbf{v}_0^\top & \mathbf{v}_1^\top & \mathbf{v}_2^\top & \dots \\ k^2 \mathbf{v}_0 & \mathbf{I}_{\chi_0} + k^2 \mathbf{N}_{\chi_0} & & & \\ \mathbf{v}_1 & & u_1(k) \mathbf{I}_{\chi_1} + \mathbf{N}_{\chi_1} & & & \\ \mathbf{v}_2 & & & u_2(k) \mathbf{I}_{\chi_2} + \mathbf{N}_{\chi_2} & & \\ \vdots & & & & & \ddots \end{bmatrix}, \quad (\text{A12})$$

where \mathbf{N}_{χ_j} is the *nilpotent symmetrized Jordan block* of size χ_j defined in Ref. [41], and

$$u_j(k) = \nu_j + \frac{|\nu_j|}{\nu_j} k^2, \quad \operatorname{Re} \nu_j > 0. \quad (\text{A13})$$

Equation (A6) then gives:

$$\mathcal{K}(k) = a + bk^2 + \sum_{n=1}^{\chi_0} c_{0,n} k^{2+2n} + \sum_{j=1}^{\chi} \sum_{n=1}^{\chi_j} \frac{c_{j,n}}{(m_j + k^2)^n}, \quad (\text{A14})$$

with

$$m_j = \frac{\nu_j^2}{|\nu_j|}, \quad c_{j,n} = -\frac{\nu_j}{|\nu_j|} \mathbf{v}_j^\top \mathbf{N}_{\chi_j}^{n-1} \mathbf{v}_j, \quad \nu_0 = 1. \quad (\text{A15})$$

Given \mathcal{K} above, minimal χ further implies

$$m_j \neq m_{j'}, \quad \forall j \neq j', \quad c_{j,\chi_j} \neq 0. \quad (\text{A16})$$

With these conditions, the parameterization in Eq. (A12) is *unique* up to the ordering of the diagonal blocks [41] and a sign choice for each \mathbf{v}_j ; similarly, Eq. (A14) is a unique parameterization of a general rational function of k^2 with numerator of degree $p \leq \chi + 1$ and denominator of degree $q = \chi - \chi_0 \leq \chi$ [40]. Within the minimal- χ assumption, at least one between p and q must be maximal. Relaxing that assumption, one concludes that first-derivative GCPEPS with χ auxiliary fields correspond to the subclass of Gaussian states whose kernel is a rational function of k^2 of (inclusive) degree $\chi + 1$ over χ , and whose poles lie outside the non-negative real axis, $k^2 \geq 0$.

A few comments are due. First, as expected, the number of parameters in \mathbf{W} and \mathcal{K} matches exactly. Second, the parameterization in Eq. (A13) is to ensure $\operatorname{Re} \mathbf{U} > 0$, so that the Gaussian integrals formally converge; however, analytically continuing Eq. (A6) to arbitrary nonsingular \mathbf{U} we can obtain the same \mathcal{K} as above simply setting

$$u_j(k) = m_j + k^2, \quad m_j \notin (-\infty, 0], \quad (\text{A17})$$

with the understanding that the path-integral contour is deformed accordingly. Finally, we comment on *typicality*: Generic rational functions \mathcal{K} have maximal degree and only simple poles; specularly, generic complex symmetric matrices $\mathbf{U}^{(0)}, \mathbf{U}^{(1)}$ are diagonalizable with distinct (i.e., simple), nonzero eigenvalues. Both conditions correspond to $\chi_0 = 0$ and $\chi_j = 1$ for all $j \geq 1$, namely a diagonal virtual block

$$\mathbf{U} = \operatorname{diag}(m_1 + k^2, \dots, m_\chi + k^2), \quad (\text{A18})$$

recovering Eq. (9) of the main text, i.e. the ansatz of Ref. [34].

Proof. That \mathbf{W} in Eq. (A12) yields \mathcal{K} in Eq. (A14) is seen immediately by inverting \mathbf{U} blockwise, using the identity:

$$[\alpha \mathbf{I}_N + \beta \mathbf{N}_N]^{-1} = \sum_{n=1}^N \alpha^{-n} \beta^{n-1} \mathbf{N}_N^{n-1}, \quad \mathbf{N}_N^0 := \mathbf{I}_N. \quad (\text{A19})$$

We already know that GCPEPS correspond to rational kernels of degree $\chi + 1$ over χ . Since Eq. (A14) parametrizes the most general such function, it is enough to show that Eq. (A15) can be solved for arbitrary $\{m_j\}$ and $\{c_{j,n}\}$. It then follows that \mathbf{W} can be written as above and that Eq. (A16) is not restrictive.

The equation for m_j is trivial, and the constraint $\operatorname{Re} \nu_j > 0 \implies \arg(m_j) \neq \pi$ only excludes poles in the $k^2 \geq 0$ axis. The equations for $c_{j,n}$ in different blocks j are independent, thus it suffices to consider a single block of arbitrary size N . For $N = 1$, obviously there are two solutions for all $c \neq 0$. For larger N , recalling $\mathbf{N} = \mathbf{N}_N$ is symmetric and cyclic [41], by the Jacobian criterion [84] one concludes that the equations

$$\mathbf{w}_k = \mathbf{v}^\top \mathbf{N}^{k-1} \mathbf{v} \quad (\text{A20})$$

are algebraically independent. Then, invoking some notions of algebraic geometry [85, 86], it can be argued that Eq. (A20) can be solved for \mathbf{v} at least for *generic* $\mathbf{w} \in \mathbb{C}^N$. Below we give a more direct proof, which shows that the measure-zero exceptional set where Eq. (A20) does not have a solution lies inside the $\mathbf{w}_N = 0$ subspace, where χ is not minimal.

\mathbf{N} is similar to the usual Jordan nilpotent [41]:

$$\mathbf{P}^{-1}\mathbf{N}\mathbf{P} = \mathbf{J} , \quad \mathbf{J}_{ij} = \delta_{i+1,j} . \quad (\text{A21})$$

Given a cyclic vector \mathbf{r} for \mathbf{N} , the similarity matrix \mathbf{P} can be constructed using as columns the Jordan chain

$$\mathbf{e}_N = \mathbf{r} , \quad \mathbf{e}_{k-1} = \mathbf{N}\mathbf{e}_k , \quad k = 1, \dots, N-1 , \quad (\text{A22})$$

In the $\tilde{\mathbf{v}} = \mathbf{P}^{-1}\mathbf{v}$ basis, Eq. (A20) reads

$$\mathbf{w}_k = \tilde{\mathbf{v}}^\top \mathbf{P}^\top \mathbf{P} \mathbf{J}^{k-1} \tilde{\mathbf{v}} . \quad (\text{A23})$$

The Gram matrix $\mathbf{P}^\top \mathbf{P}$ is lower anti-triangular (by nilpotency of \mathbf{N}), and \mathbf{J} acts on it by shifting its columns to the right. Therefore, Eq. (A23) defines a triangular system of quadratic equations, $\mathbf{w}_k = f_k(\tilde{\mathbf{v}}_k, \dots, \tilde{\mathbf{v}}_N)$, which admits a solution if all pivots are nonzero. As we show below, $\mathbf{P}^\top \mathbf{P}$ can be taken to be the exchange matrix, $(\mathbf{P}^\top \mathbf{P})_{ij} = \delta_{i+j, N+1}$. Then Eq. (A23) takes the simple form,

$$\mathbf{w}_k = \sum_{i+j=N+k} \tilde{\mathbf{v}}_i \tilde{\mathbf{v}}_j , \quad (\text{A24})$$

and we can iteratively solve for $\tilde{\mathbf{v}}$ (and thus \mathbf{v}):

$$\mathbf{w}_N = 2\tilde{\mathbf{v}}_N \tilde{\mathbf{v}}_N \neq 0 , \quad \mathbf{w}_{N-1} = 2\tilde{\mathbf{v}}_{N-1} \tilde{\mathbf{v}}_N , \quad \dots , \quad \mathbf{w}_k = 2\tilde{\mathbf{v}}_k \tilde{\mathbf{v}}_N + \sum_{k < l < N-k} \tilde{\mathbf{v}}_l \tilde{\mathbf{v}}_{N-l} , \quad \dots \quad (\text{A25})$$

The equation for $\tilde{\mathbf{v}}_N$ is quadratic while all the other are linear thus, overall, there are exactly two solutions: $\pm \tilde{\mathbf{v}}_N$.

All that is left to show is that we can choose \mathbf{r} cyclic such that $\mathbf{P}^\top \mathbf{P}$ is the exchange matrix. In general,

$$(\mathbf{P}^\top \mathbf{P})_{ij} = \mathbf{e}_i^\top \mathbf{e}_j = \mathbf{r}^\top \mathbf{N}^{2N-i-j} \mathbf{r} =: h_{i+j-N} , \quad (\text{A26})$$

is Hankel and lower anti-triangular ($h_k = 0$ for $k < 1$). If \mathbf{r} is cyclic, so is $Q(\mathbf{N})\mathbf{r}$ with

$$Q(z) = q_0 + q_1 z + \dots + q_{N-1} z^{N-1} , \quad q_0 \neq 0 . \quad (\text{A27})$$

The transformation acts transitively on the moments $\{h_k\}_{k=1}^N$, and

$$Q \cdot h_k = \mathbf{r}^\top \mathbf{N}^{N-k} Q^2(\mathbf{N}) \mathbf{r} = \sum_{i+j \leq k-1} q_i q_j h_{k-i-j} \stackrel{!}{=} \delta_{k,1} \quad (\text{A28})$$

defines an upper triangular system which can be solved iteratively, starting from $k = 0$, provided the pivots are nonzero, namely $h_1 \neq 0$. This is always guaranteed because \mathbf{N}^{N-1} is rank-1 symmetric, hence $\mathbf{N}^{N-1} = \mathbf{n}\mathbf{n}^\top$ for some $\mathbf{n} \neq 0$, thus

$$h_1 = (\mathbf{n}^\top \mathbf{r})^2 = 0 \implies \mathbf{N}^{N-1} \mathbf{r} = 0 , \quad (\text{A29})$$

which is in contradiction with \mathbf{r} being cyclic. \square

Notice that the existence of a solution to Eq. (A28) is equivalent (lifting the action of Q from \mathbf{v} -space to $\tilde{\mathbf{v}}$ -space) to the statement that a non-degenerate anti-triangular Hankel matrix is congruent to the exchange matrix through a triangular Toeplitz matrix $Q(\mathbf{J})$.

Given a rational function in the form Eq. (A14), the associated GCPEPS matrix is thus obtained solving Eq. (A15) via Eq. (A25) (given the closed-form expression for \mathbf{N} in Ref. [41], it should be even possible to compute \mathbf{P} explicitly). Conversely, a given \mathbf{W} can be put in the form of Eq. (A12) via the transformation in Eq. (A10) as follows:

- (i) Diagonalize $\mathbf{U}^{(0)} \rightarrow \mathbf{I}_\chi$ by congruence with an invertible \mathbf{R} , then eliminate $\mathbf{v}^{(0)} \rightarrow 0$ by a shift with $\mathbf{s} = -\mathbf{R}^\top \mathbf{v}^{(0)}$; both operations are possible because $\mathbf{U}^{(0)}$ is non-singular.
- (ii) Put $\mathbf{U}^{(1)}$ in symmetrized Jordan normal form [41] by a complex orthogonal rotation \mathbf{R} (residual gauge freedom); equivalently, compute the usual Jordan decomposition of $\mathbf{U}^{(1)}$ and replace each Jordan block by a symmetrized one with the same eigenvalue, as given in closed form in Ref. [41].

The virtual block then takes a block diagonal form:

$$\mathbf{U} = \mathbf{I}_\chi + \bigoplus_j [\lambda_j \mathbf{I}_{\chi_j} + \mathbf{N}_{\chi_j}] k^2. \quad (\text{A30})$$

Permute the blocks so that eventual null eigenvalues of $\mathbf{U}^{(1)}$ appear first; then repeat steps (i) and (ii) above on the remaining $j \geq \ell$ blocks, where $\mathbf{U}^{(1)}$ is non-singular — this time with the roles of $\mathbf{U}^{(0)}, \mathbf{v}^{(0)}$ and $\mathbf{U}^{(1)}, \mathbf{v}^{(1)}$ exchanged. Then,

$$\mathbf{U} = [\mathbf{I}_{\chi_0} + k^2 \mathbf{N}_{\chi_0}] \oplus \cdots \oplus [(m_\ell + k^2) \mathbf{I}_{\chi_\ell} + \mathbf{N}_{\chi_\ell}] \oplus \cdots; \quad (\text{A31})$$

i.e. the same structure as Eq. (A12) except for, possibly, (i) degenerate blocks ($\ell > 1$, geometric multiplicity $\text{gm}(m_j) > 1$), and (ii) $\text{Re } m_j \not> 0$. Provided m_j is not real negative, positive definiteness can be enforced by rotating the sub-multiplet φ_j corresponding to the j th block by a global phase

$$\varphi_j \rightarrow \sqrt{\frac{|m_j|}{m_j}} \varphi_j \quad \text{so that} \quad m_j + k^2 \rightarrow u_j(k), \quad (\text{A32})$$

with u_j as defined in Eqs. (A13) and (A15). Finally, blocks $j \neq j'$ with degenerate eigenvalues $m_j = m_{j'}$ and $\chi_j \geq \chi_{j'}$ are merged by computing the associated residues $c_{j,n}, c_{j',n'}$ via Eq. (A15), then solving Eq. (A15) with $c_{j,n} \rightarrow c_{j,n} + c_{j',n'}$ (padding the latter with zeros if $\chi_j > \chi_{j'}$) to obtain a new \mathbf{v}_j , and finally dropping the j' block.

2. Tridiagonal form & continued fractions

Generic GCPEPS matrices can, by means of Eq. (A10), be brought to tridiagonal form with constant off-diagonals:

$$\mathbf{W} = \begin{bmatrix} u_0 & i & & & \\ i & u_1 & \ddots & & \\ & \ddots & \ddots & i & \\ & & i & u_\chi \end{bmatrix}, \quad (\text{A33})$$

which depends on $2\chi + 2$ complex parameters $s_\alpha, r_\alpha \in \mathbb{C}$ via

$$u_\alpha(k) = r_\alpha k^2 + s_\alpha, \quad r_\alpha \neq 0 \text{ for } \alpha = 1, \dots, \chi. \quad (\text{A34})$$

Equation (A6) then gives

$$\mathcal{K} = u_0 + (\mathbf{U}^{-1})_{11} = u_0 + \frac{1}{u_1 + \frac{1}{\ddots + \frac{1}{u_\chi}}}, \quad (\text{A35})$$

which *uniquely* encodes a *generic* rational function of degree $\chi + 1$ over χ . Its proper part, i.e. the nontrivial GCPEPS contribution $(\mathbf{U}^{-1})_{11}$, is a (truncated) Jacobi-type continued fraction, or *J-fraction* for short [87].

Proof. That \mathbf{W} in Eq. (A33) gives rise to \mathcal{K} in Eq. (A35) was already shown in Section II, where we also argued that the latter encodes generic rational functions [43, Problem 3.11] — more precisely, those in [87, Theorem 41.1]. Uniqueness of the J-fraction follows from that of the quotient and remainder of polynomial division at each step of the Euclidean algorithm, and from $r_\chi \neq 0$, which removes “tail ambiguities”; an explicit proof is given in [87, pp. 161–162].

To put a generic \mathbf{W} in the form of Eq. (A33), we need to (i) diagonalize $\mathbf{W}^{(1)}$ and (ii) bring $\mathbf{W}^{(0)}$ to tridiagonal form. We may assume all off-diagonal elements are nonzero and can thus be rescaled to i by renormalizing ϕ_α ; if otherwise, the continued fraction terminates early and some virtual fields decouple, implying that χ is not minimal. Diagonalization of $\mathbf{W}^{(1)}$ works as in step (i) of the prescription at the end of the previous section, here applied to $\mathbf{v}^{(1)}$ and $\mathbf{U}^{(1)}$ (generically non-singular). To tridiagonalize $\mathbf{W}^{(0)}$ by a complex orthogonal rotation of the virtual fields, observe that, under congruence by $\mathbf{I}_1 \oplus \mathbf{O}$ orthogonal, a symmetric matrix \mathbf{X} transforms as

$$\mathbf{X} = \begin{bmatrix} b & \mathbf{a}^\top \\ \mathbf{a} & \mathbf{Y} \end{bmatrix} \mapsto \mathbf{X}' = \begin{bmatrix} b & \mathbf{a}^\top \mathbf{O} \\ \mathbf{O}^\top \mathbf{a} & \mathbf{Y}' \end{bmatrix}, \quad \mathbf{Y}' = \mathbf{O}^\top \mathbf{Y} \mathbf{O}. \quad (\text{A36})$$

Generically $\mathbf{a}^\top \mathbf{a} \neq 0$, in which case \mathbf{O} can be chosen such that $\mathbf{a}^\top \mathbf{O} = (a, 0, \dots, 0)$, with $a = \pm \sqrt{\mathbf{a}^\top \mathbf{a}}$ by orthogonality. The procedure is then repeated for $\mathbf{X} \leftarrow \mathbf{Y}'$, iterating until \mathbf{Y}' is one-dimensional. \square

Although here we focused on the generic case, the above prescription can be adapted to singular $\mathbf{U}^{(1)}$ — i.e., kernels with sub-maximal denominator degree — by swapping the roles of $\mathbf{W}^{(0)}$ and $\mathbf{W}^{(1)}$. The off-diagonals of \mathbf{W} in Eq. (A33) and the numerators of the continued fraction in Eq. (A35) then acquire a k^2 and k^4 factor, respectively.

Unlike Eq. (A12), $\text{Re } \mathbf{U}$ is *not necessarily positive definite* for \mathbf{W} in Eq. (A33). Unless

$$\text{Re } s_\alpha, \text{Re } r_\alpha > 0, \quad \alpha = 1, \dots, \chi, \quad (\text{A37})$$

the auxiliary-field path-integral in Eq. (A5) converges only if regarded as an appropriately tilted contour integral¹². This issue is partially cured by introducing a slightly less rigid ansatz: relaxing $\mathbf{W}_{\alpha,\alpha+1} = i$ gives the additional gauge freedom,

$$\phi_\alpha \rightarrow \sqrt{v_\alpha} \phi_\alpha, \quad v_0 = 1, \quad (\text{A38})$$

which corresponds to an equivalence transformation of continued fractions:

$$u_0 + \frac{1}{u_1 + \frac{1}{\ddots + \frac{1}{u_\chi}}} = u_0 + \frac{v_1}{v_1 u_1 + \frac{v_2}{v_2 u_2 + \ddots + \frac{v_{\chi-1} v_\chi}{v_\chi u_\chi}}}. \quad (\text{A39})$$

By it, some \mathcal{K} for which Eq. (A37) does not hold can be written in terms of a positive definite $\text{Re } \mathbf{U}$ (and thus real φ), at the expense of a redundant parameterization. However, this does not apply to all J-fractions, not even generically.

Proof. Since $v_\alpha > 0$ cannot change the signature of $\text{Re } \mathbf{U}$ (Sylvester's law of inertia), it is enough to consider phase rotations, $v_\alpha = e^{i\theta_\alpha}$. By these, whenever $s_\alpha \neq 0$ and r_α, s_α are not in counter-phase (i.e. generically), diagonal entries $\text{Re } v_\alpha u_\alpha$ can be made positive, ensuring $\text{Re } \mathbf{U}^{(1)} \succ 0$ but not necessarily $\text{Re } \mathbf{U}^{(0)} \succ 0$ (because of the off-diagonals). and one can construct examples (neither generic nor exceptional) where the latter can be enforced and vice versa. Let I_α be the interval of angles θ_α compatible with positive diagonal entries and $I_{\alpha\beta} = I_\alpha + I_\beta$:

$$I_\alpha = \{\theta_\alpha : \text{Re } v_\alpha r_\alpha, \text{Re } v_\alpha s_\alpha > 0\}, \quad I_{\alpha,\beta} = \{(\theta_\alpha + \theta_\beta) \bmod 2\pi : \theta_\alpha \in I_\alpha, \theta_\beta \in I_\beta\}; \quad (\text{A40})$$

note I_α shrinks as r_α, s_α approach counter-phase. If $0 \in I_{\alpha,\alpha+1} \forall \alpha$, the off-diagonals of $\text{Re } \mathbf{U}^{(0)}$ can be chosen purely imaginary, ensuring $\text{Re } \mathbf{U}^{(0)} \succ 0$ regardless of Eq. (A37). Conversely, if $I_{\alpha,\alpha+1} \subset (\pi - \epsilon, \pi + \epsilon)$ for some α , with

$$0 < \epsilon < \pi, \quad |s_\alpha| |s_{\alpha+1}| < \cos^2(\epsilon/2), \quad (\text{A41})$$

then

$$\text{Re}(v_\alpha s_\alpha) \text{Re}(v_{\alpha+1} s_{\alpha+1}) - \left[\text{Re}(i\sqrt{v_\alpha v_{\alpha+1}}) \right]^2 < 0, \quad (\text{A42})$$

for the $(\alpha, \alpha+1)$ principal minor of $\text{Re } \mathbf{U}^{(0)}$, and thus $\text{Re } \mathbf{U}^{(0)}$ cannot be made positive-definite. \square

Choosing $v_\alpha = r_\alpha^{-1}$ in Eq. (A38) gives $\mathbf{U}^{(1)} \rightarrow \mathbf{I}$, corresponding to monic denominators in $(\mathbf{U}^{-1})_{11}$:

$$(\mathbf{U}^{-1})_{11}(k) = \frac{1}{k^2 + s_1/r_1 - \frac{-1/r_1 r_2}{\ddots - \frac{-1/r_{\chi-1} r_\chi}{k^2 + s_\chi/r_\chi}}}. \quad (\text{A43})$$

Within this ansatz, J-fractions realizable with $\text{Re } \mathbf{U} \succ 0$ correspond to generic (truncated) *positive-definite J-fractions* [87]. This class encompasses many useful continued fraction expansions with nice and extensively studied convergence properties [87]. It partially overlaps with Eq. (A37), but neither is a subset of the other.

¹²We stress that the continued fraction expansion of $(\mathbf{U}^{-1})_{11}$ in Eq. (A35) holds regardless [42].

Proof. We first recall the definition of a positive-definite continued fraction, in the notation of Ref. [87], then show how it (generically) relates to $\text{Re } \mathbf{U} \succ 0$ by a $\pi/2$ rotation of the complex plane. Consider the J-fraction

$$(\mathbf{J}^{-1})_{11}(z) = \frac{1}{z + b_1 - \frac{a_2^2}{z + b_2 - \frac{a_3^2}{\ddots}}}, \quad (\text{A44})$$

formally originating from the expansion of the leading coefficient of the reciprocal of the infinite J-matrix [87]

$$\mathbf{J}(z) = z\mathbf{I} + \mathbf{J}^{(0)}, \quad \mathbf{J}_0 = \begin{bmatrix} b_1 & a_2 & & \\ a_2 & b_2 & a_3 & \\ a_3 & b_3 & \ddots & \\ \ddots & \ddots & \ddots & \ddots \end{bmatrix}. \quad (\text{A45})$$

Following Wall [87, Definition 16.1], $(\mathbf{J}^{-1})_{11}$ is positive-definite when the real quadratic form $\text{Im } \mathbf{J}_0$ is non-negative on eventually zero sequences:

$$\sum_{n=1}^N \text{Im}(b_n)\xi_n^2 + 2 \sum_{n=2}^N \text{Im}(a_n)\xi_{n-1}\xi_n \geq 0 \quad \forall \xi \in \mathbb{R}^N, N = 1, 2, \dots; \quad (\text{A46})$$

equivalently, when $\text{Im } \mathbf{J}_N^{(0)} \succeq 0$ for all leading principal submatrices $\mathbf{J}_N^{(0)}$ of $\mathbf{J}^{(0)}$. Among other things, this implies that if $(\mathbf{J}^{-1})_{11}$ converges for one point with $\text{Im } z > 0$, then it converges to an analytic function on the whole upper half plane [87, p.110], and all its approximants (truncations) $(\mathbf{J}_N^{-1})_{11}$ have no poles for $\text{Im } z > 0$ [87, Theorem 16.1].

Suppose \mathbf{J} defines a positive-definite J-fraction. Making the replacement $\mathbf{J} \rightarrow i\mathbf{J}$ or, equivalently,

$$z \rightarrow iz, \quad a_n \rightarrow ia_n, \quad b_n \rightarrow ib_n, \quad (\text{A47})$$

Eq. (A46) and the convergence results that follow hold with $\text{Im} \rightarrow \text{Re}$. Therefore, if $i\mathbf{U}(k) = \mathbf{J}_\chi(ik^2)$, then $\text{Re } \mathbf{U} \succeq 0$, and thus generically $\text{Re } \mathbf{U} \succ 0$, whenever $\text{Re } k^2 \geq 0$ and in particular for $k^2 \geq 0$. \square

Appendix B: Higher-order derivative CPEPS

We briefly show how, by introducing additional auxiliary fields, a CPEPS with n -order derivatives ($n > 1$) can be recast as a first-order one. Section A 1 already implies this result for GCPEPS, since it shows that any rational kernel can be realized as Eq. (A12). Below we provide an explicit prescription, reminiscent of Ostrogradsky's construction [88], which also holds for non-Gaussian CPEPS.

For simplicity, let us start with only the physical field ($\chi = 0$) and set

$$W(\phi) = \int d^d \mathbf{x} \mathcal{W}(\phi(\mathbf{x}), \nabla\phi(\mathbf{x}), \dots, \nabla^n\phi(\mathbf{x})), \quad (\text{B1})$$

where n is the true maximal derivative order for ϕ (i.e., it cannot be reduced integrating by parts). Introduce $R = \lfloor n/2 \rfloor$ auxiliary-field pairs $\{(\psi_r, \lambda_r)\}_{r=1}^R$, namely n new fields if n is even and $n - 1$ new fields if n is odd, and define the first-order functional W' (the \mathbf{x} dependence of the fields is implicit):

$$W'(\phi, \psi_1, \lambda_1, \dots, \psi_R, \lambda_R) = \int d^d \mathbf{x} \left[\mathcal{W}(\phi, \nabla\phi, \psi_1, \nabla\psi_1, \dots, \psi_R, \nabla\psi_R) + \sum_{r=1}^R \lambda_r [\psi_r - \nabla^2\psi_{r-1}] \right], \quad (\text{B2})$$

with the identification $\psi_0 = \phi$. The λ_r fields act as Lagrange multipliers, whose equations of motion enforce

$$\psi_r = \nabla^2\psi_{r-1} \iff \psi_r = \nabla^{2r}\phi, \quad (\text{B3})$$

establishing the equivalence of W' and W . When n is even, the last argument of \mathcal{W} in Eq. (B2) is absent and ψ_R can be integrated as per Eq. (3) without spoiling locality, since W' does not depend on its derivatives. The result is a CPEPS with $n - 1$ auxiliaries for even and odd n alike.

For χ initial auxiliaries, the above procedure is carried out independently for each ϕ_α , producing a CPEPS with

$$\chi' = \sum_{\alpha=0}^{\chi} n_\alpha - 1 , \quad (\text{B4})$$

n_α being the maximal derivative order of ϕ_α . The counting simplifies to $\chi' = n(\chi + 1) - 1$ for a uniform order $n_\alpha = n$.

By Eq. (B4) alone one can conclude that higher-order Gaussian CPEPS are non-generic, in the sense that they correspond to non-generic first-order GCPEPS (at least when $n_0 > 1$). Indeed, while the kernel of a GCPEPS with $\sum_{\alpha=1}^{\chi} n_\alpha = N$ has denominator degree N , Eq. (B2) rewrites it as a first-order one whose denominator degree would generically be $\chi' = N + (n_0 - 1)$. The $n_0 - 1$ degree gap corresponds to higher-order derivatives of the physical field, which do not enter the denominator because ϕ is not integrated over in Eq. (2). To see why more explicitly, consider a $\chi = 0$ GCPEPS W with

$$\mathcal{W} = \frac{1}{2} \phi P^{(n_0)}(-\nabla^2) \phi ; \quad (\text{B5})$$

namely a Gaussian state with polynomial kernel $\mathcal{K} = P^{(n_0)}$ (e.g., a Lifshitz vacuum). By Eq. (A14), the first-order GCPEPS W' in Eq. (B2) corresponds (modulo field redefinitions) to a virtual block $\mathbf{U} = \mathbf{I} + \mathbf{N}k^2$, i.e. the $j = 0$ block of Eq. (A12), which does not contribute any denominator degree because \mathbf{N} is nilpotent and thus $\det \mathbf{U} = 1$.

Appendix C: Continued fraction convergence

We collect below some convergence results for the continued fractions in Section IV B. The central object of this Appendix is the continued fraction representation of $\sqrt{1+z}$ with modified χ th convergent

$$C_\chi(z, w) = 1 + \cfrac{z}{2 + \cfrac{z}{2 + \cfrac{z}{\ddots + \cfrac{z}{2 + w}}}} . \quad (\text{C1})$$

Direct inspection reveals that the continued fractions from the rational and imaginary-time evolution approximations in Eqs. (22) and (31) are affinely equivalent to it — i.e., their convergents are related by an affine transformation to C_χ :

$$\omega_\chi(k) = m C_\chi \left(z = \frac{k^2}{m^2}, w = 0 \right) , \quad \omega_{N,\epsilon}(k) = \frac{s}{\epsilon} C_N \left(z = -\frac{1}{s^2}, w = \frac{s_1}{s} - 2 \right) + \frac{s_0 - s}{\epsilon} . \quad (\text{C2})$$

A closed-form expression for C_χ follows from standard techniques for periodic continued fractions [44, Lemma 1.1]. The continuants (numerators and denominators of the convergents) satisfy the linear recurrence

$$K_\chi = 2K_{\chi-1} + zK_{\chi-2} , \quad (\text{C3})$$

with characteristic roots $\lambda_\pm = 1 \pm \sqrt{1+z}$. Its general solution takes the form

$$K_\chi = c_+ \lambda_+^\chi + c_- \lambda_-^\chi , \quad (\text{C4})$$

and c_\pm are set by the initial conditions: $K_0 = 1$, $K_1 = 2 + z$ for the numerator and $K_0 = 1$, $K_1 = 2$ for the denominator. Simplifying, we obtain

$$C_\chi(z, w) = \sqrt{1+z} \frac{1 + \eta^{\chi+1} + (w/\lambda_+)(1 + \eta^\chi)}{1 - \eta^{\chi+1} + (w/\lambda_+)(1 - \eta^\chi)} , \quad \eta = \frac{\lambda_-}{\lambda_+} = \frac{1 - \sqrt{1+z}}{1 + \sqrt{1+z}} , \quad (\text{C5})$$

which converges geometrically to $\sqrt{1+z}$ for all $w \neq -\lambda_+$, as long as $|\eta| < 1$, namely,

$$\lim_{\chi \rightarrow \infty} C_\chi(z, w) = C_\infty(z) = \sqrt{1+z} \quad \forall z > -1, w + 1 + \sqrt{1+z} \neq 0 . \quad (\text{C6})$$

Convergence is not uniform: it is faster when $|\eta| \ll 1$ ($z \rightarrow 0$) and slows down as $|\eta| \rightarrow 1^-$ ($z \rightarrow -1^+, \infty$).

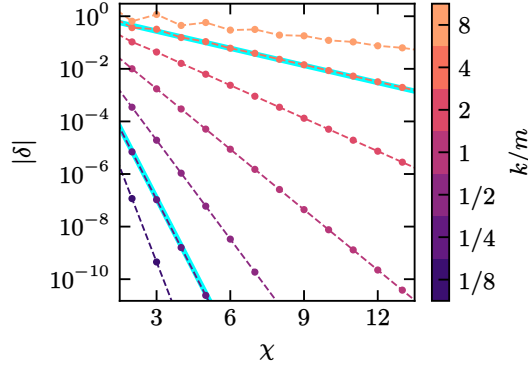


FIG. 6: Pointwise convergence of Klein-Gordon's rational approximant ω_χ in Fig. 2a. Each color refers to the magnitude of the relative deviation of $\omega_\chi(k)$ from $\omega(k)$ for one value of k/m , as a function of χ . The expansions in Eq. (C10) (cyan) are accurate already for $k/m \in \{1/4, 4\}$. Dashed lines are guides to the eye.

1. Rational approximation from Eq. (22)

In this case, $w = 0$ and C_χ simplifies significantly, yielding

$$\omega_\chi = \omega \frac{1 + \eta^{\chi+1}}{1 - \eta^{\chi+1}}. \quad (\text{C7})$$

The asymptotes in Eq. (41) are easily recovered expanding around $z = \infty$ at fixed χ via

$$\eta^n \sim (-1)^n (1 - 2n/\sqrt{z}). \quad (\text{C8})$$

For every finite k/m , $|\eta| < 1$ and thus the continued fraction converges. The relative truncation error reads

$$\delta = \frac{\omega_\chi - \omega}{\omega} = \frac{2}{1/\eta^{\chi+1} - 1} \sim 2\eta^{\chi+1}, \quad (\text{C9})$$

and has an alternating sign ($\eta \leq 0$), as expected for a positive continued fraction [44, Theorem 3.12]. From the analysis below Eq. (C6), it follows that convergence is slower for small masses and large momenta, as illustrated in Fig. 6. The following expansions hold:

$$|\delta| \sim \begin{cases} 2(k/2m)^{2(\chi+1)} & k \ll m \\ 2e^{-2(\chi+1)m/k} & k \gg m \end{cases}. \quad (\text{C10})$$

2. Imaginary-evolution approximation from Eq. (31)

This case is slightly more subtle because the derivation changes depending on whether the $\chi \rightarrow \infty$ limit is taken keeping ϵ or T fixed. Fixing $\epsilon > 0$, as in the main text, Eq. (C6) applies straightforwardly and, recalling the values of s and s_1 from Table I, we conclude that the continued fraction converges to the result in Eq. (32) for all k — provided $m > 0$, as expected. Fixing T , on the other hand, s and s_1 acquire a dependence on χ through $\epsilon = T/\chi$. Consequently, Eq. (C6) (which assumes z, w constant) does not apply. Instead,

$$\lim_{\chi \rightarrow \infty} [\eta(\chi)]^\chi = e^{-2T\omega} \neq 0; \quad (\text{C11})$$

thus

$$\lim_{\chi \rightarrow \infty} \omega_{\chi, T/\chi} = \omega \coth(T\omega). \quad (\text{C12})$$

The exact dispersion is finally recovered taking the $T \rightarrow \infty$ limit.

[1] F. Verstraete *et al.*, Matrix product states, projected entangled pair states, and variational renormalization group methods for quantum spin systems, *Adv. Phys.* **57**, 143 (2008).

[2] R. Orús, A practical introduction to tensor networks: Matrix product states and projected entangled pair states, *Ann. Phys.* **349**, 117 (2014).

[3] I. Cirac *et al.*, Matrix Product States and Projected Entangled Pair States: Concepts, Symmetries, and Theorems, *Rev. Mod. Phys.* **93**, 045003 (2021), arxiv:2011.12127.

[4] P. Silvi *et al.*, The Tensor Networks Anthology: Simulation techniques for many-body quantum lattice systems, *SciPost Physics Lecture Notes* **8**, (2019), arXiv:1710.03733.

[5] M. C. Bañuls, Tensor Network Algorithms: a Route Map, *Annu. Rev. Condens. Mat. P.* **14**, 173 (2023), arxiv:2205.10345.

[6] L. Accardi, Topics in quantum probability, *Phys. Rep.* **77**, 169 (1981).

[7] M. Fannes *et al.*, Finitely correlated states on quantum spin chains, *Comm. Math. Phys.* **144**, 443 (1992).

[8] S. R. White, Density Matrix Formulation for Quantum Renormalization Groups, *Phys. Rev. Lett.* **69**, 2863 (1992).

[9] S. Östlund and S. Rommer, Thermodynamic Limit of Density Matrix Renormalization, *Phys. Rev. Lett.* **75**, 3537 (1995).

[10] U. Schollwöck, The density-matrix renormalization group in the age of matrix product states, *Ann. Phys. January 2011 Special Issue*, **326**, 96 (2011).

[11] F. Verstraete and J. I. Cirac, Renormalization algorithms for Quantum-Many Body Systems in two and higher dimensions (2004), arXiv:cond-mat/0407066.

[12] W.-Y. Liu *et al.*, Accurate Simulation of the Hubbard Model with Finite Fermionic Projected Entangled Pair States, *Phys. Rev. Lett.* **134**, 256502 (2025).

[13] Y.-Y. Shi *et al.*, Classical simulation of quantum many-body systems with a tree tensor network, *Phys. Rev. A* **74**, 022320 (2006).

[14] G. Vidal, Entanglement Renormalization, *Phys. Rev. Lett.* **99**, 220405 (2007).

[15] V. Giovannetti *et al.*, Quantum Multiscale Entanglement Renormalization Ansatz Channels, *Phys. Rev. Lett.* **101**, 180503 (2008).

[16] M. C. Bañuls *et al.*, The mass spectrum of the Schwinger model with matrix product states, *J. High Energy Phys.* **2013** (11), 158.

[17] M. Troyer and U.-J. Wiese, Computational Complexity and Fundamental Limitations to Fermionic Quantum Monte Carlo Simulations, *Phys. Rev. Lett.* **94**, 170201 (2005).

[18] M. C. Bañuls *et al.*, Simulating lattice gauge theories within quantum technologies, *Eur. Phys. J. D* **74**, 165 (2020), arXiv:1911.00003.

[19] A. Kelman *et al.*, Gauged Gaussian projected entangled pair states: A high dimensional tensor network formulation for lattice gauge theories, *Phys. Rev. D* **110**, 054511 (2024).

[20] G. Magnifico *et al.*, Tensor networks for lattice gauge theories beyond one dimension, *Communications Physics* **8**, 322 (2025).

[21] S. Dürr *et al.*, Ab Initio Determination of Light Hadron Masses, *Science* **322**, 1224 (2008).

[22] J. B. Kogut, The lattice gauge theory approach to quantum chromodynamics, *Rev. Mod. Phys.* **55**, 775 (1983).

[23] F. Verstraete and J. I. Cirac, Continuous Matrix Product States for Quantum Fields, *Phys. Rev. Lett.* **104**, 190405 (2010).

[24] G. De las Cuevas *et al.*, Continuum limits of matrix product states, *Phys. Rev. B* **98**, 174303 (2018).

[25] J. Haegeman *et al.*, Calculus of continuous matrix product states, *Phys. Rev. B* **88**, 085118 (2013).

[26] M. Ganahl *et al.*, Continuous Matrix Product States for Quantum Fields: An Energy Minimization Algorithm, *Phys. Rev. Lett.* **118**, 220402 (2017).

[27] B. Tuybens *et al.*, Variational Optimization of Continuous Matrix Product States, *Phys. Rev. Lett.* **128**, 020501 (2022).

[28] D. Jennings *et al.*, Continuum tensor network field states, path integral representations and spatial symmetries, *New J. Phys.* **17**, 063039 (2015).

[29] J. Haegeman *et al.*, Entanglement Renormalization for Quantum Fields in Real Space, *Phys. Rev. Lett.* **110**, 100402 (2013).

[30] A. Tilloy and J. I. Cirac, Continuous tensor network states for quantum fields, *Phys. Rev. X* **9**, 021040 (2019).

[31] T. Shachar and E. Zohar, Approximating relativistic quantum field theories with continuous tensor networks, *Phys. Rev. D* **105**, 045016 (2022).

[32] G. Roose and E. Zohar, Continuum limit of gauged tensor network states (2025), arXiv:2511.10189.

[33] D. Blanik *et al.*, Internal structure of gauge-invariant projected entangled pair states, *J. Phys. A: Math. Theor.* **58**, 065301 (2025).

[34] T. D. Karanikolaou *et al.*, Gaussian continuous tensor network states for simple bosonic field theories, *Phys. Rev. Research* **3**, 023059 (2021).

[35] J. Haegeman *et al.*, Applying the Variational Principle to (1 + 1)-Dimensional Quantum Field Theories, *Phys. Rev. Lett.* **105**, 251601 (2010).

[36] V. Stojevic *et al.*, Conformal data from finite entanglement scaling, *Phys. Rev. B* **91**, 035120 (2015).

[37] A. Tilloy, Relativistic continuous matrix product states for quantum fields without cutoff, *Phys. Rev. D* **104**, 096007 (2021).

[38] A. Tilloy, Variational method in relativistic quantum field theory without cutoff, *Phys. Rev. D* **104**, L091904 (2021).

[39] N. Schuch *et al.*, Gaussian matrix product states (Edizioni della Normale, 2008) pp. 129–142, arxiv:1201.3945.

[40] European Mathematical Society, Rational function, in *Encyclopedia of Mathematics* (EMS Press, 2025).

[41] D. Ž. Đoković and K. Zhao, Tridiagonal normal forms for orthogonal similarity classes of symmetric matrices, *Linear Algebra Appl.* **384**, 77 (2004).

[42] R. A. Usmani, Inversion of Jacobi's tridiagonal matrix, *Comput. Math. Appl.* **27**, 59 (1994).

[43] T. Sauer, Rational functions as continued fractions of polynomials, in *Continued Fractions and Signal Processing* (Springer International Publishing, 2021) pp. 67–98.

[44] L. Lorentzen and H. Waadeland, *Continued Fractions: Convergence Theory* (Atlantis Press, 2008).

[45] D. Perez-Garcia *et al.*, PEPS as unique ground states of local Hamiltonians, *Proc. Spie.* **8**, 650 (2008), arxiv:0707.2260.

[46] D. S. Rokhsar and S. A. Kivelson, Superconductivity and the Quantum Hard-Core Dimer Gas, *Phys. Rev. Lett.* **61**, 2376 (1988).

[47] E. Fradkin and J. E. Moore, Entanglement Entropy of 2D Conformal Quantum Critical Points: Hearing the Shape of a Quantum Drum, *Phys. Rev. Lett.* **97**, 050404 (2006).

[48] C. Boudreault *et al.*, Entanglement and separability in continuum Rokhsar-Kivelson states, *Phys. Rev. Research* **4**, 033251 (2022), arxiv:2110.04290.

[49] E. Ardonne *et al.*, Topological order and conformal quantum critical points, *Ann. Phys.* **310**, 493 (2004).

[50] J. Alexandre, Lifshitz-type quantum field theories in particle physics, *Int. J. Modern Phys. A* **26**, 4523 (2011).

[51] K. G. Wilson and J. Kogut, The renormalization group and the ϵ expansion, *Phys. Rep.* **12**, 75 (1974).

[52] Y. Nakayama, Scale invariance vs conformal invariance, *Phys. Rep.* Scale invariance vs conformal invariance, **569**, 1 (2015).

[53] C. Holzhey *et al.*, Geometric and Renormalized Entropy in Conformal Field Theory, *Nucl. Phys. B* **424**, 443 (1994), arxiv:hep-th/9403108.

[54] E. Witten, APS Medal for Exceptional Achievement in Research: Invited article on entanglement properties of quantum field theory, *Rev. Mod. Phys.* **90**, 045003 (2018).

[55] H. Casini and M. Huerta, Entanglement entropy in free quantum field theory, *J. Phys. A: Math. Theor.* **42**, 504007 (2009), arxiv:0905.2562.

[56] T. He *et al.*, Entanglement Entropy in Lifshitz Theories, *SciPost Phys.* **3**, 034 (2017).

[57] S. A. Gentle and S. Vandoren, Lifshitz entanglement entropy from holographic cMERA, *J. High Energy Phys.* **2018** (7), 13.

[58] M. R. Mohammadi Mozaffar and A. Mollabashi, Entanglement in Lifshitz-type quantum field theories, *J. High Energy Phys.* **2017** (7), 120.

[59] J. K. Basak *et al.*, Massless Lifshitz field theory for arbitrary z , *J. High Energy Phys.* **2024** (5), 284.

[60] P. Calabrese and J. Cardy, Entanglement Entropy and Quantum Field Theory, *J. Stat. Mech: Theory Exp.* **2004**, P06002 (2004), arxiv:hep-th/0405152.

[61] B. Hsu *et al.*, Universal entanglement entropy in two-dimensional conformal quantum critical points, *Phys. Rev. B* **79**, 115421 (2009).

[62] T. Zhou *et al.*, Entanglement entropy and mutual information of circular entangling surfaces in the 2 + 1-dimensional quantum Lifshitz model, *J. Stat. Mech: Theory Exp.* **2016**, 093101 (2016).

[63] P. Bueno and W. Witczak-Krempa, Bounds on corner entanglement in quantum critical states, *Phys. Rev. B* **93**, 045131 (2016).

[64] A. Tilloy, A study of the quantum Sinh-Gordon model with relativistic continuous matrix product states (2022), arxiv:2209.05341.

[65] K. Tiwana *et al.*, A relativistic continuous matrix product state study of field theories with defects (2025), arxiv:2501.09797.

[66] K. Tiwana and A. Tilloy, Multi-Field Relativistic Continuous Matrix Product States (2025), arxiv:2511.20762.

[67] P. M. Stevenson, Gaussian effective potential: Quantum mechanics, *Phys. Rev. D* **30**, 1712 (1984).

[68] P. M. Stevenson, Gaussian effective potential. II. $\lambda\phi^4$ field theory, *Phys. Rev. D* **32**, 1389 (1985).

[69] L. Polley and D. E. L. Potter, *Variational Calculations in Quantum Field Theory* (WORLD SCIENTIFIC, 1988).

[70] G. Vidal, Efficient Simulation of One-Dimensional Quantum Many-Body Systems, *Phys. Rev. Lett.* **93**, 040502 (2004).

[71] F. Verstraete *et al.*, Matrix Product Density Operators: Simulation of Finite-Temperature and Dissipative Systems, *Phys. Rev. Lett.* **93**, 207204 (2004).

[72] J. Haegeman *et al.*, Time-Dependent Variational Principle for Quantum Lattices, *Phys. Rev. Lett.* **107**, 070601 (2011).

[73] C. M. Hurvich and C.-L. Tsai, Regression and time series model selection in small samples, *Biometrika* **76**, 297 (1989).

[74] Y. Huang and W. F. McColl, Analytical inversion of general tridiagonal matrices, *J. Phys. A: Math. Gen.* **30**, 7919 (1997).

[75] A. Franco-Rubio and G. Vidal, Entanglement and correlations in the continuous multi-scale entanglement renormalization ansatz, *J. High Energy Phys.* **2017** (12), 129.

[76] N. Vardian, Entanglement renormalization of the class of continuous matrix product states, *Phys. Rev. D* **108**, 094029 (2023), arxiv:2208.14827.

[77] J. Angel-Ramelli *et al.*, Entanglement entropy in generalised quantum Lifshitz models, *J. High Energy Phys.* **2019** (8), 72.

[78] J. Angel-Ramelli *et al.*, Logarithmic negativity in quantum Lifshitz theories, *J. High Energy Phys.* **2020** (9), 11.

[79] S. Khoshdoodi *et al.*, Capacity of entanglement in Lifshitz theories, *Phys. Rev. D* **112**, 026027 (2025).

[80] L. Vanderstraeten *et al.*, Tangent-space methods for uniform matrix product states, *SciPost Physics Lecture Notes* **7**, (2019).

[81] R. P. Feynman, Difficulties in Applying the Variational Principle to Quantum Field Theories (WORLD SCIENTIFIC, 1988) pp. 28–40.

[82] J. Zinn-Justin, *Quantum Field Theory and Critical Phenomena*, 5th ed., International Series of Monographs on Physics (Oxford University Press, 2021).

[83] J. Gallier, Schur complements and applications, in *Geometric Methods and Applications* (Springer, 2011) pp. 431–437.

[84] M. Beecken *et al.*, Algebraic independence and blackbox identity testing, *Inform. and Comput.* **222**, 2 (2013), arxiv:1102.2789.

[85] G. Lowther, When are complex polynomial maps almost surjective?, MathOverflow (2011).

[86] J. S. Milne, *Algebraic geometry (v6.10)* (2024).

[87] H. S. Wall, *Analytic Theory of Continued Fractions* (D. Van Nostrand, 1948).

[88] R. P. Woodard, The theorem of ostrogradsky (2015), arxiv:1506.02210.